LUND UNIVERSITY

Master of Science Thesis
HT2021

Polymer gel dosimetry - Using MRI-readout, simplified relatively non-toxic mixing procedure tested on FLASH

Maria Blomstedt

Supervisors

Sofie Ceberg, Christian Jamtheim Gustafsson, Crister Ceberg, Sven Bäck, Lund

This work has been conducted at
the Medical Radiation Physics,Malmö

Medical Radiation Physics, Lund
Faculty of Science
Lund University
www.msf.lu.se

GELDOSIMETRI - FÖRENKLAD
TILLVERKNINGSPROCEDUR OCH BESTRÅLNING MED FLASH

När en ny strålbehandlingsteknik ska introduceras krävs verifiering av metoden och för detta krävs dosimetrar med hög spatial upplösning och att dosen kan mätas i tre dimensioner. En potentiell dosimeter för denna applikation är polymer geldosimetern som, precis som krävs, har hög spatial upplösning i tre dimensioner. Polymer geldosimetern är en dosimeter som består av gelatin och kemikalier som uppvisar ändringar när den exponeras för strålning. En av egenskaperna som förändras kan detekteras med magnetresonanskamera (MR). Geldosimeterns fördelaktiga egenskaper är att den är vävnads ekvivalent, har hög noggrannhet och reproducerbarhet, kan integrera dosen i 3D över hela behandlingstiden och är oberoende av energi och infallsvinkel på strålningen. En av de nya strålbehandlingsteknikerna idag där det finns önskemål om en oberoende, högupplöst 3D-detektor är FLASH. En teknik där elektronstrålningen levereras med mycket högre dos per tidsenhet än normalt vid strålbehandling, över 40 Gy/s. För att få perspektiv på denna siffra kan det nämnas att normalt är dos per tidsenhet för en behandling runt 0,08 Gy/s, alltså 500 gånger lägre än vid FLASH.

SYFTE

Tidigare har tillverkningen av geldosimetrar varit väldigt tidskrävande och komplicerad då det kräver tillgång till ett labb, en utläsningsteknik, en syrefri miljö, avjoniserat vatten samt då visst innehåll är relativt giftigt. Syftet med detta examensarbete var därför att starta upp ett geldosimetrilaboratorium på universitetssjukhuset i Lund och att undersöka möjligheten att skapa en geldosimeter som har linjär dosrespons med relativt giftfria ingredienser och en förenklad tillverkningsprocedur. Den förenklade tillverkningsproceduren syftar till att kunna tillverka gelen i normala syrenivåer samt att använda vanligt kranvatten i stället för avjoniserat vatten. Ett ytterligare syfte var att undersöka om den tillverkade gelen kunde användas för verifiering av FLASH.

METOD

I det uppstartade labbet tillverkades polymer gelen bestående av vanligt kranvatten, gelatin från grishud, den relativt mindre giftiga monomeren N-isopropylamide (NIPAM), ämnet som gör att tillverkningen kan ske i normala syrenivåer tetrakis-hydroxymethyl-phosphonium-chloride (THPC) och tvärbindaren N,N'-methylene-bis-acrylamide (BIS). Gelen bestrålades till olika dosnivåer med tre olika strålslag; 220 kV fotoner, 10 MeV elektroner med konventionell dos per tidsenhet och FLASH. Efter bestrålningen skedde utläsningen av den absorberade dosen med MR.

RESULTAT OCH DISKUSSION

Arbetet visar att det är möjligt att tillverka en geldosimeter som har linjär dosrespons med relativt giftfria ingredienser och förenklad tillverkningsprocedur. Gelen uppvisade mindre skillnader inom samma omgång gel när den strålades med lågenergetiska fotoner vilket tyder på god reproducerbarhet. Större skillnader observerades mellan olika omgångar gel när den bestrålades med samma stråltyp, vilket understryker behovet som finns att varje omgång gel behöver kalibreras. Gelen uppvisade linjäritet av dosresponsen upp till minst 23 Gy för alla strålslag som undersöktes.

Abstract

Background: One of the polymer gel dosimeters available today is the N-isopropylamide (NIPAM) polymer gel dosimeter which has a less toxic monomer compared to other polymer gels and the advantage of being able to be manufactured under normal oxygen levels. Polymer gel dosimeters in general are advantageous independent dosimeters to use for verification of new radiation treatment techniques due to its favorable qualities such as very high resolution, 3D coverage, tissue equivalence and independence of energy and incident direction of the radiation beam. One of the new and upcoming treatment techniques today where there is a desire for an independent, high resolution 3D detector is FLASH, an irradiation technique where the radiation is delivered using ultra high dose rate of 40 Gy/s or more.

The aim of this thesis was to start up a gel dosimetry laboratory and to investigate the feasibility of creating a NIPAM gel dosimeter with linear dose response using magnetic resonance imaging (MRI) readout, using relatively non-toxic ingredients and a simplified mixing procedure. An additional aim was to investigate the gel dose response when irradiated with FLASH.

Method: NIPAM polymer gels were manufactured using tap water and concentrations of 5 % w/w (weight concentration) gelatin from porcine skin, 3 % w/w NIPAM, 3 % w/w N,N'-methylene-bis-acrylamide (BIS) and 21-26 mM tetrakis-hydroxymethyl-phosphonium-chloride (THPC). Vials containing the gel were irradiated with either 220 kV photons, 10 MeV electrons at conventional doe rates, or FLASH about 24 h after manufacturing. The vials were irradiated with doses up to around 40 Gy. The gel dose response was assessed through its R2 relaxation rate by acquiring T2 weighted MRI images of the vials approximately 24 h after irradiation. The doses delivered to the vials were calculated based on previous output measurements made on the specific machine or measured using film dosimetry.

Results: The results show that intra-batch variations, with respect to the dose response reproducibility, are small with a standard deviation (SD) of the R2 relaxation rate between 0.010-0.021 s^{-1} for doses up to 10 Gy and with R2 values between 1.405 and 2.231 s^{-1}. However, inter-batch variations are significantly larger with relative difference up to 19 %. The gel exhibits linearity ($R^2 \geq 0{,}98$) of the dose response up to 28 Gy when irradiated with 220 kV photons, up to 23 Gy when irradiated with 10 MeV electrons at conventional dose rates and up to 27 Gy when irradiated with FLASH. Additionally, the results indicate a lower gel dose response when irradiated with FLASH compared to irradiation with 220 kV photons or 10 MeV electrons at conventional dose rates.

Conclusions: It is feasible to use relative non-toxic ingredients (NIPAM), MRI-readout and a simplified mixing procedure with tap water and under normal levels of oxygen to obtain a gel dosimeter with linear dose response. The small intra-batch variations indicate very high dose response reproducibility while the larger inter-batch variations underline the need for calibration of each gel batch. The gel exhibited linearity of the dose response up to 23 Gy for all three radiation beam types used. A lower gel dose response was observed when irradiated with FLASH compared to irradiation with 220 kV photons or 10 MeV electrons at conventional dose rates.

Table of contents

1 Introduction

The goal of radiotherapy is to kill cancer cells while minimizing the impact on surrounding normal tissue. In other words, this means to cover the target volume with the prescribed dose while the dose to the surrounding normal tissue is kept as low as possible [1]. For each individual patient a 3D simulation of the treatment is made, a dose plan, which in theory meets these requirements. To verify the dose plan, the absorbed dose distribution is measured in three dimensions. The dosimeters primary used for this today consist of diodes or ionization chambers situated in an array or two orthogonal arrays which unfortunately normally measure the dose in 1D or 2D only and thus has limitations in the 3D spatial resolution [1] [2]. To obtain a complete 3D distribution with these detector systems estimations must be made from a limited number of measured points. The limitation in spatial resolution is due to the distance between the measurement points, typically 5-10 mm in the plane, which means that the ionization is integrated over an area or a volume. Furthermore, correction factors e.g., for the detectors non-soft tissue equivalence, energy dependency, beam incident direction must be incorporated in the calculations of the measured absorbed dose.

Despite the mentioned limitations these dosimeters and detector systems are used daily for verification of dose plans since the result is obtained fast and is accurate enough. However, when verifying new treatment techniques higher spatial resolution and 3D coverage is highly desirable, especially since the new and upcoming techniques are becoming more advanced and complex. One potential dosimeter for this application is the polymer gel dosimeter since this dosimeter has favorable qualities such as high resolution and 3D coverage [1]. Additionally, it is also soft tissue equivalent and independent of energy and incident direction of the radiation beam [1] [3] [4]. When polymer gels are exposed to radiation, polymerization occurs which results in changed characteristics of the gel [1]. These changes can be measured and readout with different readout techniques, one of which is magnetic resonance imaging (MRI).

The use of gel for dosimetry purposes was first proposed in the 1950s and since then the technique has been greatly developed and improved [5]. Polymer gel dosimeters, which is the most widely used 3D gel dosimeters, were introduced as early as 1954 [5] [6]. The reason why polymer gels are not implemented for daily clinical use is foremost due to that there are toxic content in the gel and due to the relatively large time required from production to the readout [1] [2] [5]. In general, the time required is above 50 hours. One example of where polymer gels have already been used is in the verification of Volumetric Modulated Arc Therapy (VMAT) in the beginning of the 21st century [4]. New and upcoming treatment techniques today where gel dosimetry could be advantageous for verification is for example breathing adapted tomotheray and FLASH.

2 Aim

The aim was to start up a gel dosimetry laboratory and to investigate the feasibility of creating a gel dosimeter with linear dose response using relatively non-toxic ingredients (NIPAM), MRI-readout, as well as a simplified mixing procedure i.e., tap water and under normal levels of oxygen. Additionally, the aim was to investigate the gel dose response when irradiated with FLASH.

3 Background

3.1 NIPAM polymer gel dosimeters

There exists numerous of different polymer gel dosimeters today and a few examples of such dosimeters are PAG, BANG, MAGIC and BANANA [1]. The beneficial properties of polymer gel dosimeter are the high spatial resolution, 3D coverage, soft tissue equivalence, sufficient accuracy, good reproducibility, integration of dose during the whole treatment time and high dose sensitivity [1] [3] [4]. Furthermore, they are also independent of energy (in major parts of the important energy range) and incident direction of the radiation beam. In this master thesis the polymer gel dosimeter that will be utilized is one called NIPAM, which is the abbreviation for N-isopropylamide.

Beyond the advantageous characteristics of gel dosimeters just described, NIPAM gels also contain a less toxic monomer with a lower possibility of passing through the human skin or being inhaled [6], characteristics obviously favorable when manufacturing and handling the gel. Nevertheless, safety precautions such as using a fume hood, goggles and gloves when manufacturing the NIPAM gel must be made. Other, less favorable characteristics of the NIPAM gel, is that it is expensive, linear energy transfer (LET) dependent, highly affected if oxygen contamination occurs and the response is dependent of how the radiation is fractioned [1] [2] [6]. In recent published papers there is a disagreement whether the gel is dependent of the dose rate or not [2] [4]. In the paper published by Waldenberg et al. it is argued that a higher dose rate results in lower dose response [2].

Polymer gel dosimeters in general consists of deionized water, monomers, gelatin and crosslinkers [6]. The monomer in NIPAM dosimeters is N-isopropylamide and the crosslinker is N,N'-methylene-bis-acrylamide (BIS). NIPAM gels also consist of the oxygen scavenger tetrakis-hydroxymethyl-phosphonium-chloride (THPC) in very small amounts. This compound is classified as acute toxic and hazardous for the environment which contributes to the importance of manufacturing the gel in a safe manner. THPC extorts all the oxygen that is dissolved in the gel during the manufacturing process which is crucial since the peroxides, otherwise created by the oxygen, prevents polymerization to occur [3]. Before THPC was introduced to the world of gel dosimetry, the production of the gels was much more complicated since it had to be done in oxygen-free environments. Gels which are produced under normal levels of oxygen, like the NIPAM gel, are called normoxic gels. Additionally, THPC also reduces the amount of long-lived free radicals in the gel [6]. Long-lived free radicals together with volatile non polymerized monomers can give rise to polymerization at other positions than at the actual position of the exposure, which obviously can lead to false results and should therefore be avoided. However, THPC does not solve the problem if oxygen leaks into the gel between the production and the irradiation of the gel. Therefore, it is important to use materials for the phantoms which have low oxygen permeability [3].

The course of events when polymer gel dosimeters are exposed to ionizing radiation is initially that radiolysis takes place [3] [5], a process in the water in which free radicals and ions are created. The free radicals interact with the monomers and induce polymerization, meaning that the monomers are coupled together to chains called polymers. The polymers together with the crosslinkers forms stable networks which are held in place by the gelatine, thus enabling to maintain spatial information about the exposure [6]. The stable networks give rise to changes in some of the characteristics of the gel i.e., in the R2 relaxation rate, mass density, elasticity,

and opacity which can be readout with MRI, x-ray Computed Tomography, ultrasonography, and optical scanning respectively [1]. The most commonly used readout technique is MRI [3].

3.2 MRI in polymer gel dosimetry

In Magnetic Resonance Imaging (MRI) there are mainly two factors that contributes to the contrast in the image [7]. These two factors are variations in proton density, i.e., water content, and variations in magnetic relaxation rate. The latter one refers to the process in which excited magnetic hydrogen nuclei returns to the equilibrium distribution after being excited by a radio frequency (RF) pulse. There are two types of magnetic relaxation mechanisms with individual relaxation times; the longitudinal spin-lattice relaxation time T1, and the transversal spin-spin relaxation time T2 [8]. T1 is a measure of how fast excited nuclei returns to the ground state and how fast the longitudinal net magnetization, M_z, increases in the z direction (direction of the main magnetic field) and returns to its original state. T2 relaxation is instead a measure of how fast the spins dephase in the xy-plane (perpendicular to the main magnetic field), which describes how fast the net magnetization M_{xy} in the transversal plane diminishes.

MR images can be either T1 weighted, T2 weighted, or proton density weighted depending on whether differences in T1, T2 or proton density is featured in the image [7]. By varying and combining the repetition time (TR) and the echo time (TE) in the MRI data acquisition any of these weightings can be obtained, where TR is the time between two consecutive excitations and TE is the time from the excitation to when the echo signal is collected. To obtain a T2 weighted image both the TR and TE need to be long, which in this context refers to around 2000-2500 ms and 70-120 ms respectively [9]. When TR is long, the longitudinal net magnetization is allowed to fully recover to its original state for most anatomical structures which means that differences in T1 are not featured. When TE is long, the dephasing of the transversal net magnetization becomes noticeable and differences in T2 is featured.

As mentioned, one of the induced changes in a gel caused by radiation can be studied using MRI. Specifically, the change in the gel is reflected by a change in the R2 relaxation rate, which is given by

$$R2 = \frac{1}{T2}. \quad (1)$$

The MRI signal, S, decays monoexponentially with time and is given by

$$S = S_0 e^{-TE*R2}, \quad (2)$$

where S_0 is the signal at time zero [3].

There are different types of pulse sequences that can be used for acquiring MR images. When quantifying T2, fast spin echo (FSE) is an advantageous alternative [10]. Other names of this pulse sequence are Turbo Spin Echo (TSE) and Rapid Acquisition with Relaxation Enhancement (RARE). With FSE, several spin echoes are generated after each excitation, i.e., after each 90° RF pulse, by applying several equally spaced RF refocusing pulses of 180° after the excitation. The obtained spin echoes are acquired as separate phase-encoding lines in k-space, normally arranged in a periodic fashion with empty phase-encoding lines in between each generated line. By repeating the pulse sequence, and by altering the amplitudes of the phase-encoding gradients, all phase-encoding lines in k-space can be obtained and subsequently

reconstructed into one MR image. The number of echoes collected after each excitation i.e., the number of 180° refocusing pulses, is called Echo Train Length (ETL). With FSE, different echo times are represented in the k-space data [10]. Therefore, instead of talking about one TE for a FSE sequence, the term effective echo time (TE_{eff}) is used. TE_{eff} is the TE of the echo acquired as the phase-encoding line in the center of k-space, which is where the image contrast information of the MR image is represented. To obtain images with different TE_{eff} and thus different T2 weighted image contrasts, FSE sequences with different TE_{eff} are acquired. R2 can be quantified using FSE sequences by acquisition of MR images at multiple TE_{eff} and fit the obtained signal and TE_{eff} to the monoexponential model in equation (2) as

$$S = S_0 e^{-TE_{eff} * R2}. \quad (3)$$

R2 is affected when the gel is exposed to radiation due to the fact that the stable network of crosslinked polymers that are formed makes the protons in the gel less movable [11] [12]. In turn, the less movable protons lead to increased correlation time, which is the time required for the protons to move over a molecular distance in the medium or to change orientation. Consequently, larger correlation times lead to shorter T2 relaxation time, see Figure 1 [8]. This means that when the absorbed dose is increased a decrease in the signal in a T2 weighted MR image can be observed. Since R2 is the inverse of T2, R2 becomes larger with increased absorbed dose.

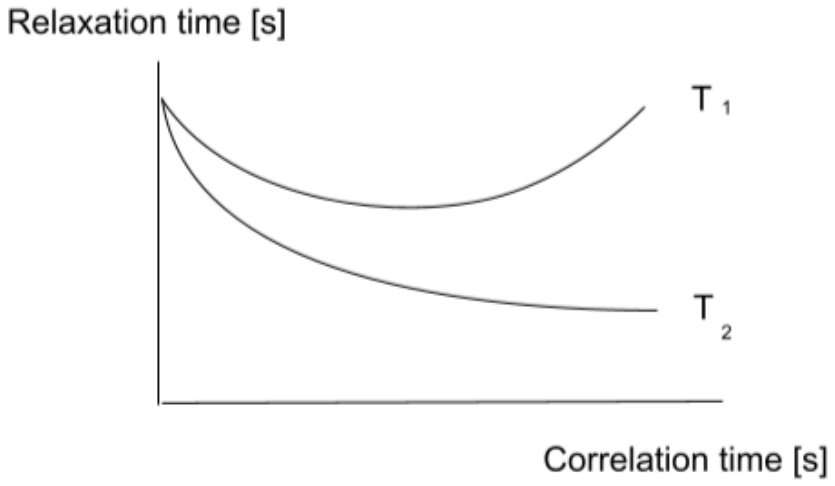

Figure 1: Relaxation times T1 and T2 as a function of correlation time. Image inspired by figure 1 in the article made by J.Demangeat [8]

3.3 Film dosimetry

The principle of film dosimetry is based on the transmission of light through a processed film [17]. The transmission depends on the film opacity, i.e., how impervious the film is, which is measured in optical density, OD. OD is defined as

$$OD = \log \frac{I_0}{I}, \quad (4)$$

where ideally I_0 is the intensity of the transmitted light through an unirradiated film and I the intensity of the transmitted light through the irradiated film. In reality, it is the gray scale values that are being quantified and thus used in the equation instead of the light intensity. The gray scale values can be measured for example with a scanner and beyond dependency on the light intensity, the gray scale values can depend on e.g., non-linearity and variations of light response of the scanner. To be able to convert the OD to dose, the film must be calibrated which is done by irradiation of the film with known doses at ISO center. By measuring the OD and relating it to the known doses, a calibration curve is obtained.

Within film dosimetry, radiochromic films are most widely used [17]. Radiochromic films are based on radiochromic reactions which are reactions defined as being triggered by ionizing radiation and resulting in changed color of the radiation sensitive medium. When exposed to ionizing radiation chain-growth photopolymerization is induced in the film which, as previously explained, means that monomers are coupled together to chains called polymers. Here, the polymers formed has a blue color which becomes darker with increasing absorbed dose. However, before irradiation, radiochromic films are translucent. After exposure the polymerization proceed for about 24 h after which the color stabilizes. Due to this, the transmitted light intensity of the film is usually measured after equally many hours. The darkening of the film is proportional to the absorbed dose and therefore by measuring transmission of light through the film, analogous with the darkening of the film, the absorbed dose can be obtained.

3.4 The cabinet irradiatior XenX – 220 kV photons

XenX is the name of a research-based rotational X-ray cabinet irradiator, mainly used to irradiate cells and small animals [13]. The XenX (Figure 2) is much smaller than a conventional linear accelerator (linac) but still has many of the desirable properties such as a 360 degrees rotating gantry, x-ray imaging, collimators, and an adapted dose planning system. At the XenX a 220 kV x-ray beam is used which is low in comparison to most clinical linacs which have a voltage of around 4-20 MV. The dose rate at the XenX is approximately 1 Gy per 19 sec at ioscenter, the point where the beams intersect if the gantry is rotated, when irradiating a cell bottle.

3.5 FLASH – ultra high electron dose rate

FLASH is the name of the irradiation technique where electron radiation is delivered with ultra-high dose rate, above 40 Gy/s [14]. To put this number into perspective the dose rate at conventional treatments is around 5 Gy/min or 0.08 Gy/s. With ultra-high dose rate, the amount

Figure 2: The cabinet irradiator XenX

of radiation induced toxicities in normal tissue is decreased, compared to normal treatment methods, while tumor control is still obtained [14], an effect referred to as the FLASH effect. The explanation for why this effect occurs has not been determined with complete certainty, but the most promising and spread-out hypothesis is that the radiation causes oxygen depletion in the normal tissue which makes it more radiation resistant. Nevertheless, this hypothesis does not explain why tumor cells are not affected in the same way which thus indicates that oxygen depletion is not the whole truth behind the FLASH effect. Additional to the FLASH effect, FLASH irradiation also possesses the advantage of having a short treatment time, in the range of 0.1 s and shorter [15]. Theoretically, this short treatment time could result in a decrease, or potentially removal, of the probability of intra-fraction motions and thus resulting in a better and more precise treatment.

In most studies made on FLASH, the ultra-high dose rate is given with an electron beam from a prototype research linear accelerator [16]. Because of the high costs and limited access to these accelerators, research has been made on how to instead update a clinical linear accelerator and make it able to deliver FLASH. The research was successful and today it is possible to make such updates to deliver FLASH. This type of updates has been made at Skåne University Hospital, Lund on an ELEKTA Precise (ELEKTA AB, Stockholm, Sweden) clinical linear accelerator [15]. Since FLASH is such a novel irradiation technique no proper dose monitoring system yet has been developed yet. Therefore, FLASH irradiation is given with only one large open field and verified, for example, with film dosimeters and potentially in the future with gel dosimeters.

4 Materials and method

4.1 Manufacturing of the NIPAM gel

The manufacturing process of the gel was carried out in a fume cupboard under normal oxygen levels and during the whole process a protective coat, protective goggles, and latex gloves were used.

Tap water was heated in a large open container to a temperature of 45 °C and the magnetic stirrer, which was on during the whole remaining manufacturing process, was started. The combined heating and stirring device was an IKA® C-MAG HS 7 control. The gelatine was added slowly to the heated water and when the gelatine was completely dissolved NIPAM and BIS were added. To avoid photopolymerization the steps of adding the polymers and until the manufacturing process was completed, was performed in the darkest environment possible. The mixture was let to cool down to 38 °C and then THPC was added. The concentration of the components mixed into the tap water were 5 % w/w gelatin from porcine skin (gel strength 300 type A, Sigma-Aldrich), 3 % w/w NIPAM (97 % Sigma-Aldrich), 3 % w/w BIS (99 % Sigma-Aldrich), between 21 and 26 mM THPC (80 % solution in water, Sigma-Aldrich). By weight, the amount of THPC were in all experiments 2.0 g because the readability of the scale used was 1.0 g. The gel mixture was poured down into 15 ml circular vials.

4.2 Irradiation

Independently of how the gel was irradiated the vials were all stored in the dark in room temperature (around 21 °C) for about 24 h before they were irradiated. This step was conducted to avoid exposure of ambient light to the gels, which again otherwise could induce photopolymerization, and such that the gel would have time to set. In all experiments, the vials were irradiated one at a time and otherwise kept in their cardboard holder.

4.2.1 Dose response reproducibility assessment

To thoroughly analyze the dose response reproducibility, the gel was irradiated with photons at the XenX with a 220 kV beam, 13.0 mA current, broad focus and a 2 mm Cu filter. The vials were irradiated axially with open fields placed 2 cm from and parallel to the central axis in a fixation mounted on a Solid Water (SW) phantom block. An ionization chamber was placed at 1 cm depth in the SW phantom 2 cm from the central axis but on the opposite side of the axis relative the vials. The ion chamber was used to verify linearity of the machine. The SW phantom was placed such that the horizontal laser was at the surface of the phantom, resulting in SSD 33 cm since SSD to the laser is 35 cm and the vial is 2 cm in diameter. The setup is schematically illustrated in figure 3. An additional SW phantom beneath the referred SW phantom to avoid backscatter was not used due to the risk that the XenX irradiator platform sags or bends. The calculated dose rate to the vials with this setup was 1 Gy per 19 seconds. The relative placement of the laser crossing the vials axially, the vials themselves, and the ion chamber, was such that the laser crossed the middle of the vials and the tip of the ion chamber. Seven vials were irradiated for each dose at 0.5, 2, 5 and 10 Gy respectively.

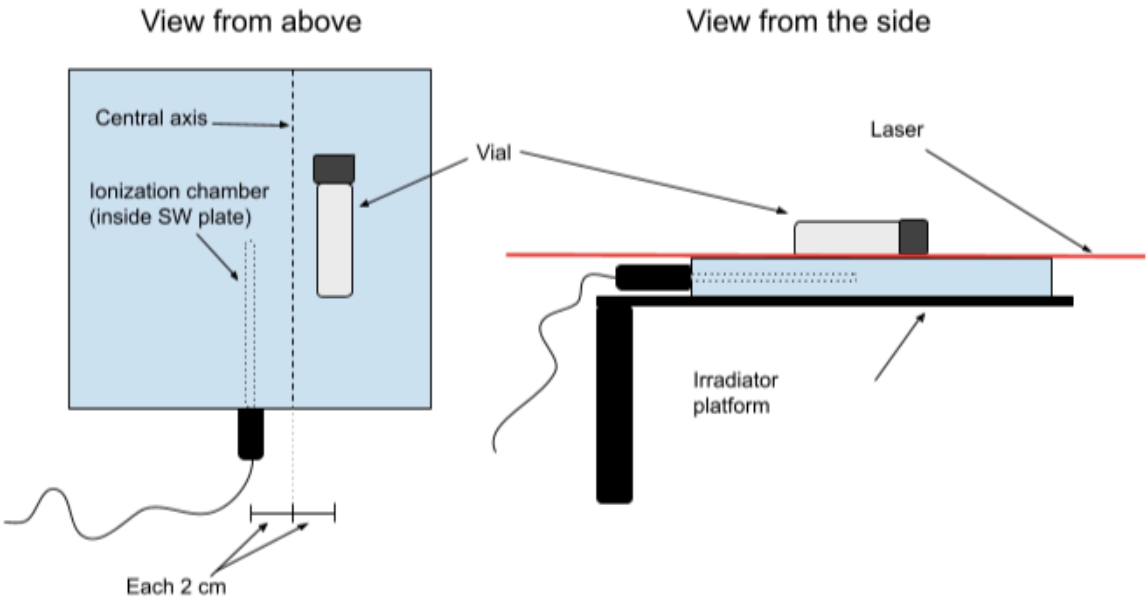

Figure 3: Schematic illustration of the setup used for the dose response reproducibility assessment irradiation

4.2.2 Dose response assessment for various beam types and dose rates

One batch of gel was irradiated only with 220 kV photons, a second batch with 10 MeV electrons at conventional dose rate and FLASH and a third batch with 220 kV photons, 10 MeV electrons at conventional dose rate, and also FLASH. For the first two batches, two vials were irradiated at the same dose level for respective radiation beam type and for the third batch only one vial was irradiated. The irradiation scheme for all batches can be seen in Table 2 section 5.4.

4.2.2.1 FLASH

The gel was irradiated with a 10 MeV electron FLASH beam at the updated clinical ELEKTA Precise linac at Skåne Unversity Hospital (Figure 4). The vials were irradiated 2 cm from the central axis in a fixation. On top of the vials, a 5 mm thick bolus was placed as an attempt to keep the whole vial within the plateau of the electron depth dose curve. An ionization chamber was placed at 5 cm depth in the SW phantom, also 2 cm from the central axis but on the opposite side of the axis relative the vials. The ionization chamber was placed at this depth in order to be situated in the bremsstrahlung tail of the electron depth dose curve. A Cerrobend plate was placed on the applicator with a 10x10 cm opening. When irradiating with FLASH, this linac is controlled on a pulse level with a dose of around 2-3 Gy/pulse depending on the setup used. When irradiating the vials, the source to surface distance, SSD, was 65 cm resulting in approximately 2 Gy per pulse. The maximum pulse repetition frequency is 200 Hz which with the used setup means a dos rate of around 400 Gy/s. A detailed description of the updates and modifications made on this specific linac to make it able to deliver FLASH radiation can be found in the article made by Lempart et al. [15].

4.2.2.2 10 MeV electrons with conventional dose rate

The gel was irradiated with a 10 MeV electron beam with conventional dose rate at the same linac as when irradiated with FLASH. The exact same setup and settings were used in the two cases except that the ion chamber and the bolus were not used in the case of the electron beam with conventional dose rate, and the beam was then controlled in MU.

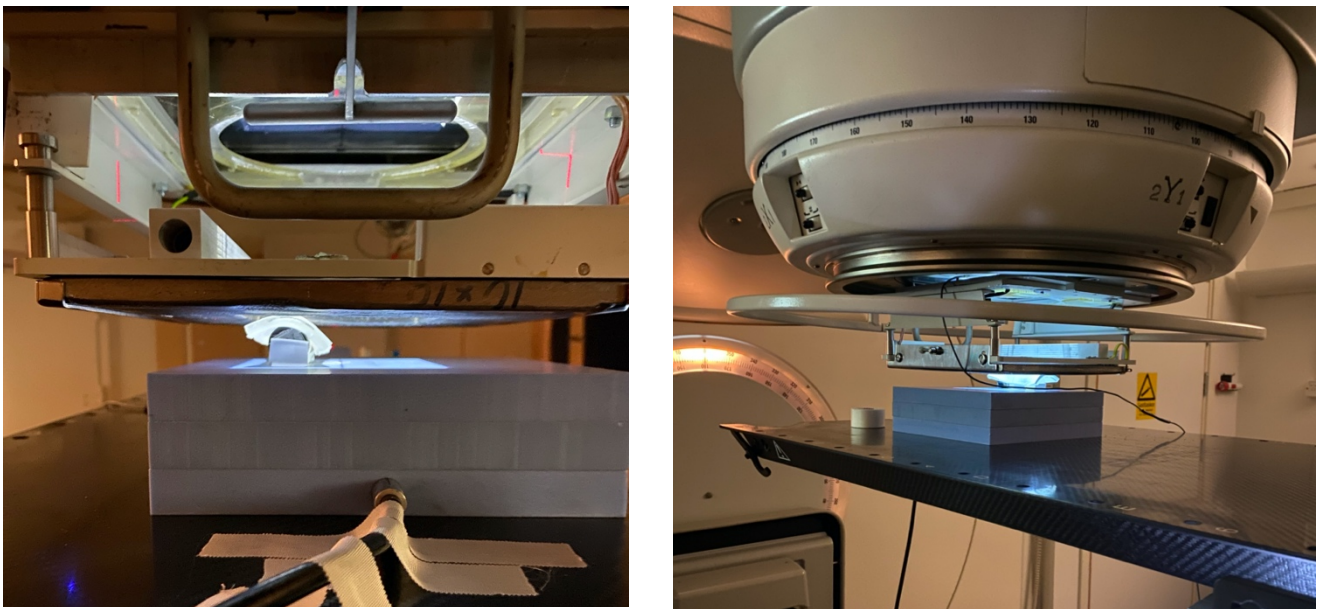

Figure 4: The setup used when irradiating with FLASH. The same setup was used to irradiate with 10 MeV electrons at conventional dose rates but without the bolus on top of the vial

4.2.2.3 220 kV photons

The irradiation with 220 kV photons was made at the XenX with the same settings and setup as previously described when irradiating with 220 kV photons.

4.2.3 Film dosimetry

Radiochromic film was used to measure an approximate dose to the gel vials when irradiated with FLASH and 10 MeV electron beam with conventional dose rate. Small pieces of film, about the same size as the internal dimension of the vials, were wrapped in plastic wrap and put into separate water-filled vials. The vials were irradiated one at a time at the same position as the gel-filled vials had been irradiated and such that the film inside the vials would be perpendicular to the beam. The vials were irradiated with 3, 7, 11 and 17 pulses respectively when using FLASH and with 291, 679, 1068 and 1650 MU when using the 10 MeV electron beam with conventional dose rate.

The radiochromic film used was GafChromic XD, which is a film optimated for doses around 10 Gy. The films were scanned using a flatbed scanner (Epson Expression 12000XL; Seiko Epson Corporation, Nagano, Japan). The calibration curve of the film was given with dose as a function of 10^{OD}. The average intensity of ROIs covering approximately half the area of the scanned films were made in ImageJ. The doses were then found using the calibration curve and equation (4). Linear relationships of dose as a function of number of pulses and MU respectively was obtained.

4.3 MRI signal readout and data processing

Before the MRI signal readout was conducted, the vials were stored at the same dark spot as before the irradiation but now for about 23 h. Again, the vials were stored in the dark to avoid exposure of ambient light to the gels and hence to avoid induced photopolymerization. The vials were moved to the MRI scanner room at least 1 h before the MRI signal readout for the

gel to reach MRI room temperature equilibrium. This was an important preparation step of the process since R2 is temperature dependent.

The vials were scanned at a General Electric (GE) Architect 3T MR scanner while still in their cardboard holder, see Figure 5 to the left and Figure 6 to the right. They were scanned with a 30 channels anterior array light weight GE Air coil placed on top of the cardboard holder and the posterior spine 40 channels integrated coil underneath, see Figure 5. Sixteen images with different TE_{eff} were acquired using a FSE pulse sequence where each individual scan provided data for one TE_{eff}. Between each new TE_{eff} scan, a manual prescan was conducted, enabling the individual TE images to be acquired with the same MR signal gain. The images were acquired in the coronal plane, i.e., providing cross sections of all the vials at the same time. The time settings used were: TR 4000 ms, and sixteen TE_{eff} of 14.4 ms, 86.5 ms, 158.7 ms, 245.2 ms, 317.3 ms, 389.4 ms, 461.6 ms, 533.7 ms, 620.2 ms, 692.4 ms, 764.5 ms, 836.6 ms, 908.7 ms, 995.3 ms, 1067 ms and 1140 ms. Other settings used for the FSE sequence were ETL 80, one slice, acquisition matrix size 512x512, bandwidth 122 Hz/pixel, anatomical region setting pelvis/pelvis, FOV in frequency-encoding direction 20.0 cm (superior-inferior in the image), FOV in phase-encoding direction 20.0 (left-right in the image) cm, and in plane pixel acquisition size 0.4x0.4 mm with a slice thickness of 10 mm. The placement of the center of the slice was approximately one third from the bottom of the vial in all experiments, see placement in Figure 6 to the right. More detailed acquisition parameter settings can be found in Figure 7.

The TR of 4000 ms, sixteen TE_{eff} and the longest echo time of 1140 ms was chosen to match the settings used in previous work made on polymer gel dosimetry with MR as the readout technique [2] [12]. The additional settings were adjusted to best fit these desired parameters and to minimize susceptibility-, truncation- and wrap-around artifacts.

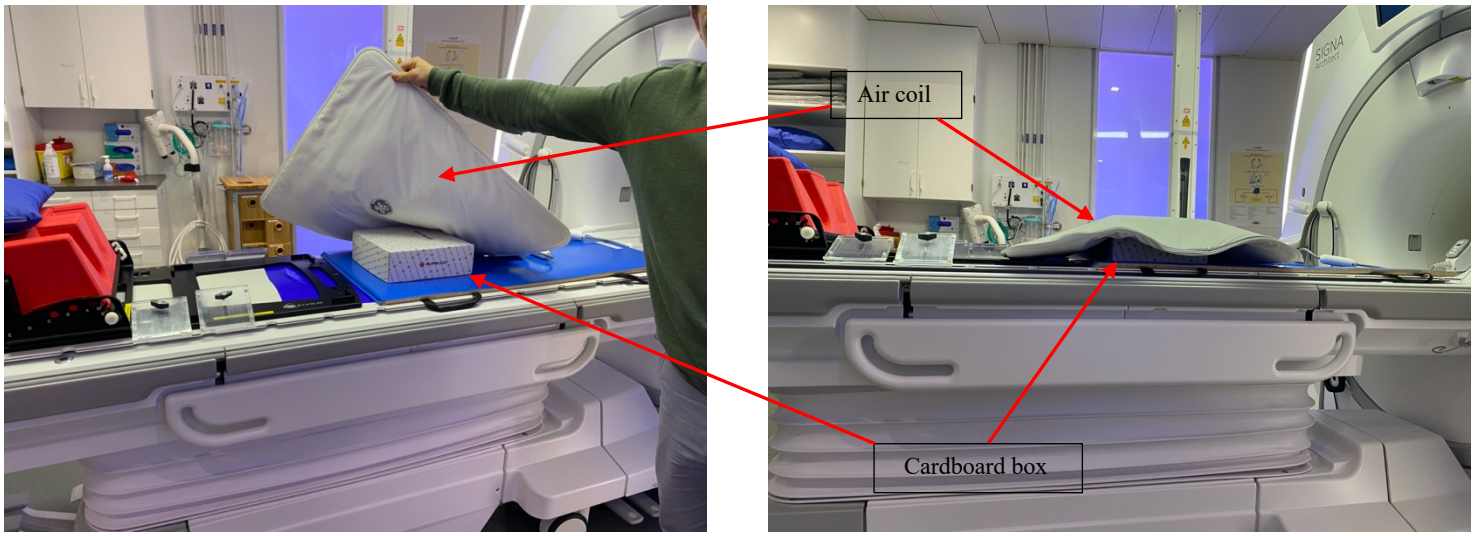

Figure 5: To the left, the cardboard holder containing the vials and the light weight GE Air coil. To the right, the actual placement of the cardboard box and air coil during scanning

Figure 6: To the left, vials in the cardboard holder seen from above. To the right, the approximate placement of the slice in the experiments

The MR images for each experiment were analyzed using the free version of MICE Toolkit 2021.2.1 https://micetoolkit.com and excel version 16.56. A screenshot of the layout in MICE Toolkit is shown in Figure 8 to the left. A ROI for each vial was drawn in MICE and the placement and size of the ROIs were about the same in all experiments (Figure 8, to the right). The ROIs were placed with some distance from the edges of the vials to avoid including the vial glass and to exclude any truncation artifacts appearing near the vial edges in some of the images. The same ROIs were used in all MR images within one experiment since all the images had the same frame of reference. For all vials, the average pixel intensity in each ROI, in each MR image was extracted and exported to excel. The average pixel intensity as a function of TE_{eff} was plotted for all vials. In the plot, a monoexponential curve fit using trend line function was made to obtain the R2 value, the model is provided in equation (3). The R2 values were subsequently plotted as a function of dose. Linearity of R2 as a function of dose was evaluated using R^2 by including an increasing number of data points, from the lowest to higher, until a value of < 0.98 was obtained.

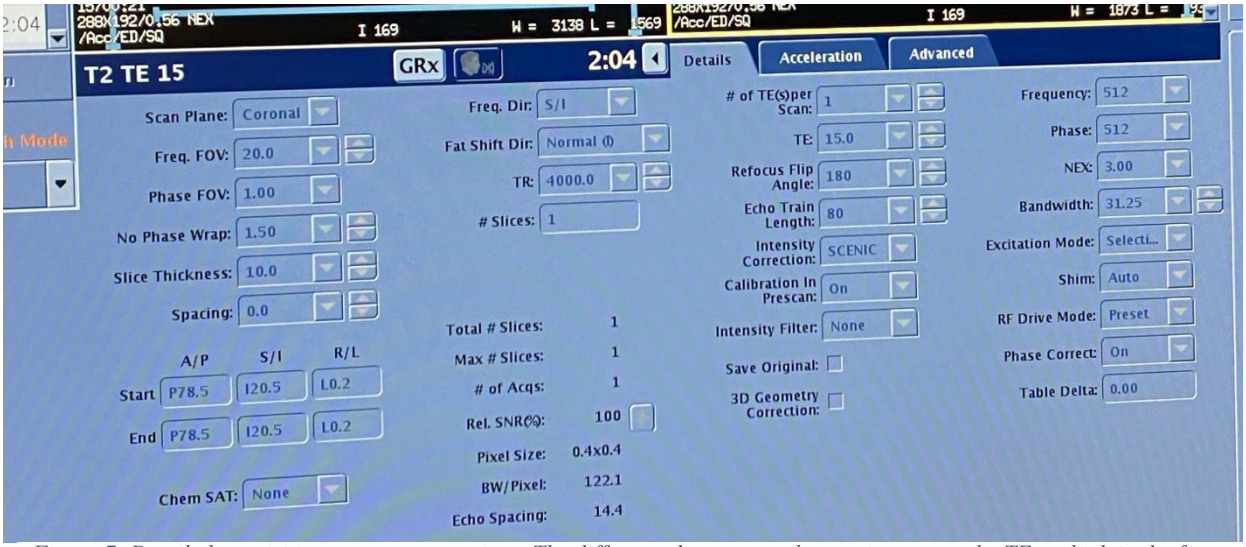

Figure 7: Detailed acquisition parameters settings. The difference between each experiment was the TE_{eff} which in the figure is represented by TE

To validate the R2 values and the described approach of obtaining them, R2 values were also calculated using a second approach utilizing a T2 map generated in MICE. A T2 map was generated automatically in MICE through fitting of data from the MR images with multiple echo times to the model provided in equation (3). The average T2 values in each vial were obtained using the same ROIs as previously. The average T2 values were inverted to find the R2 values. The reason why the latter, slightly simpler approach, was not used for all experiments instead of the first approach is because it does not generate the plot of pixel intensity as a function of TE_{eff} for the user to observe. Instead, it only generates the T2 map immediately.

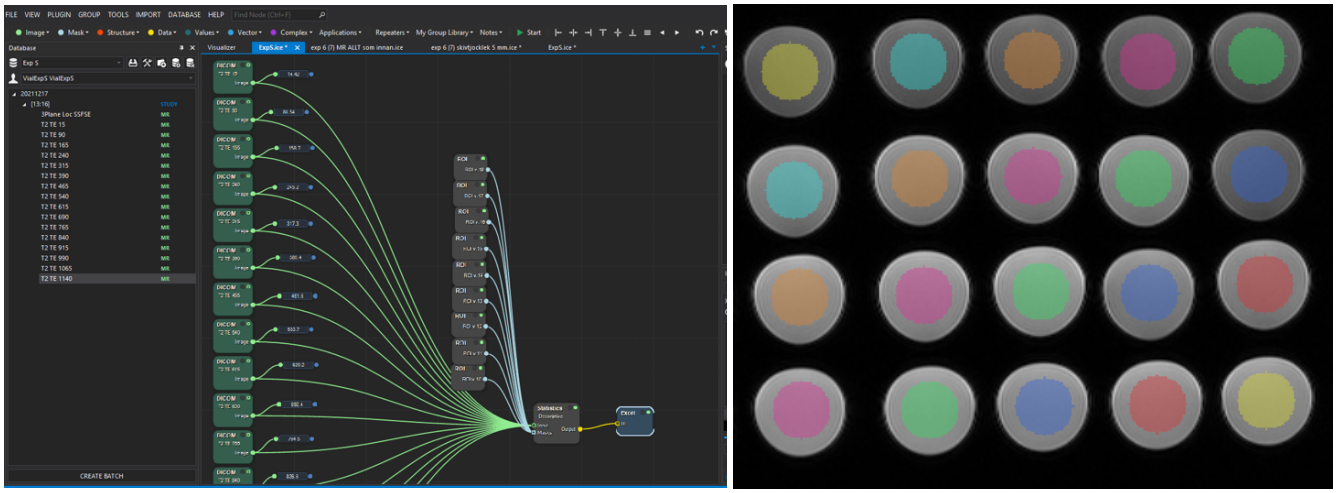

Figure 8: To the left, a screenshot of the layout in MICE Toolkit. To the right, example of the ROIs placement inside the vials on the MR images.

5 Results

5.1 Pixel intensity MR images

To visualize a typical example of MR images at various echo times for the gel dosimetry experiments carried out within this study, sixteen MR images at different TE_{eff} (14.4, 86.5, 158.7, 245.2, 317.3, 389.4, 461.6, 533.7, 620.2, 692.4, 764.5, 836.6, 908.7, 995.3, 1067, and 1140 ms) from one of the experiments are presented in Figure 9. The resulting pixel intensity of nine of the vials in all MR signal images as a function of TE_{eff} is plotted in Figure 10. In the small, attached MR image in the same figure, Figure 10, it is indicated with numbers (1-9) which nine vials it concerns. The vials are numbered with increasing dose and the doses they received are presented in column 2 in Table 3. The exponential curve fits made to obtain the R2 values are also included in Figure 10.

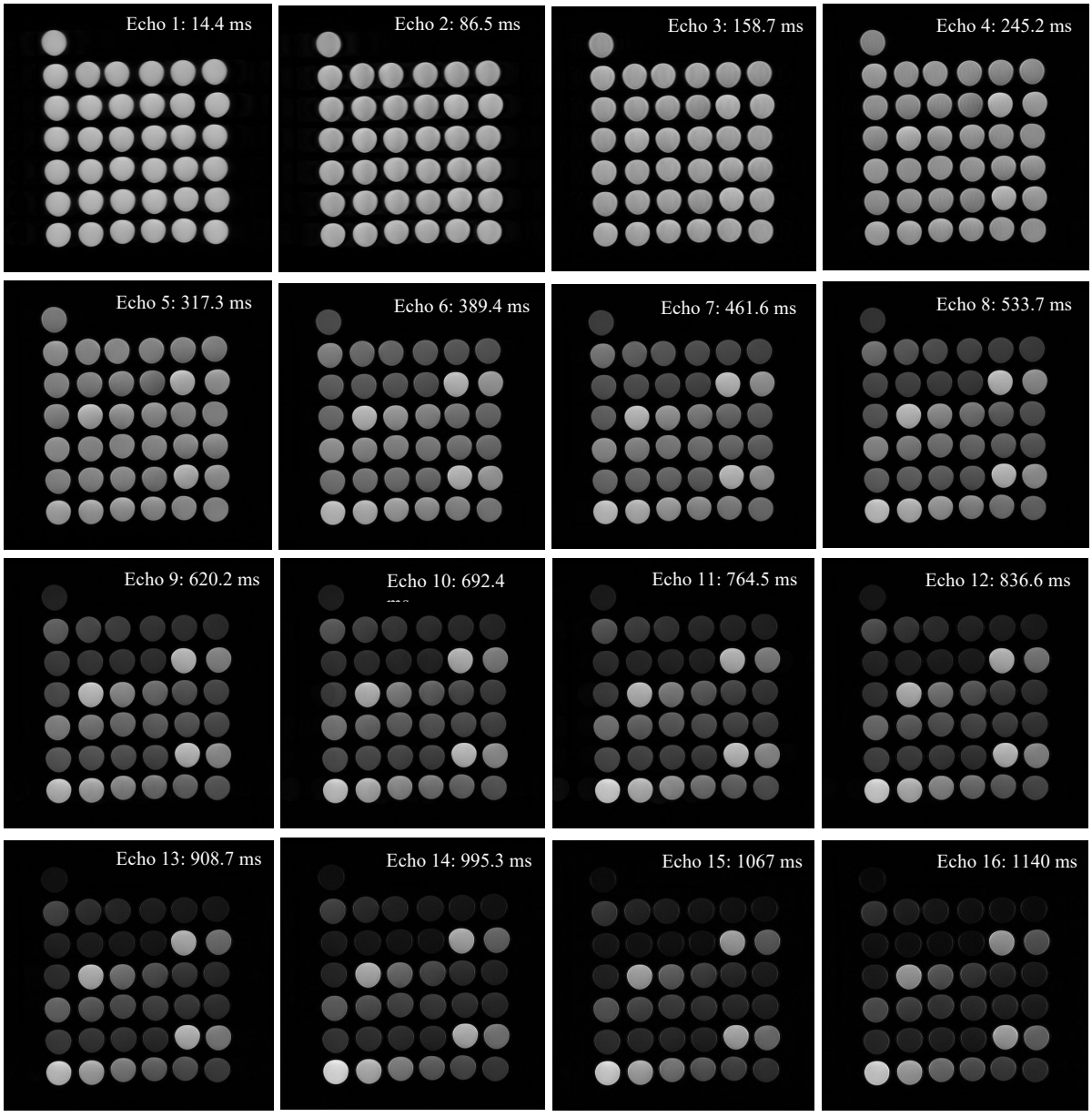

Figure 9: Sixteen MR images at different TE_{eff} with the same frame of reference and vials

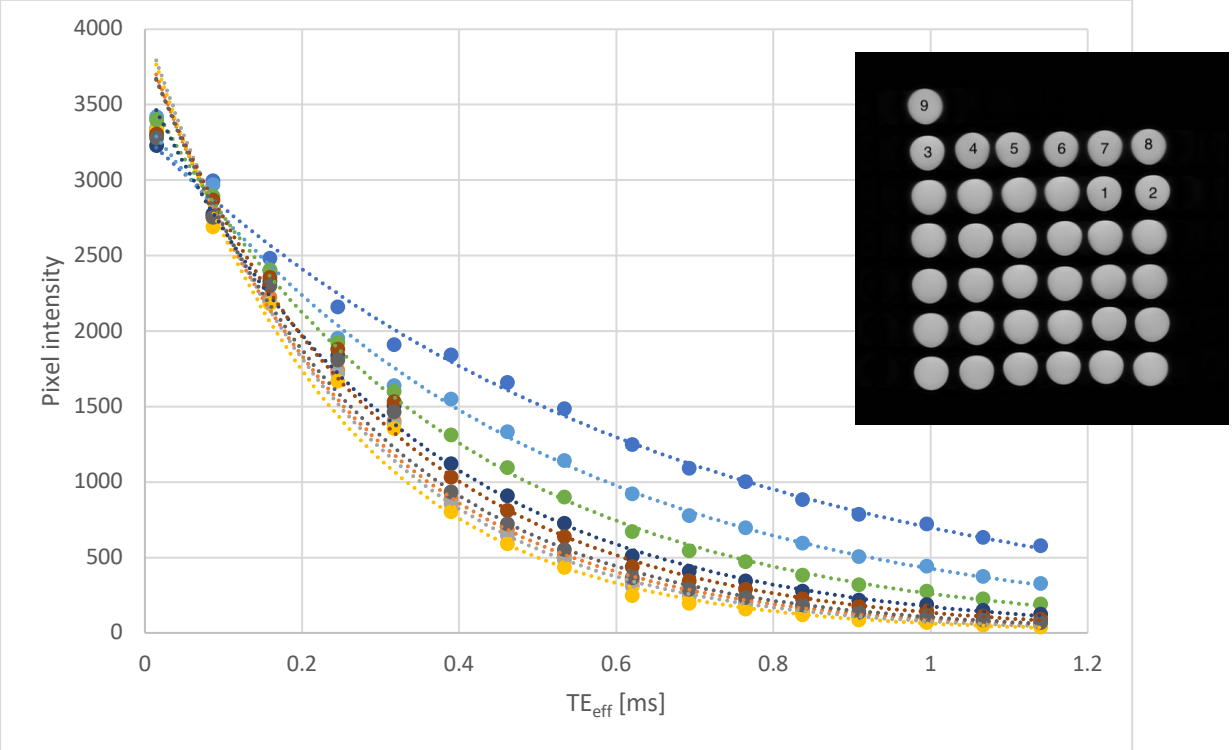

Figure 10: Example of pixel intensity as a function of TE_{eff} for the nine vials indicated with black dots in the attached MR image.

5.2 Doses film dosimetry

The result from irradiation of radiochromic film placed in water filled vials is presented in Figure 11. The vials were irradiated with 3, 7, 11, and 17 pulses respectively when using FLASH and with 291, 679, 1068, and 1650 MU when using 10 MeV electrons at conventional dose rates. The calibration curves shown in Figure 11 were used to find the doses given to the gel filled vials.

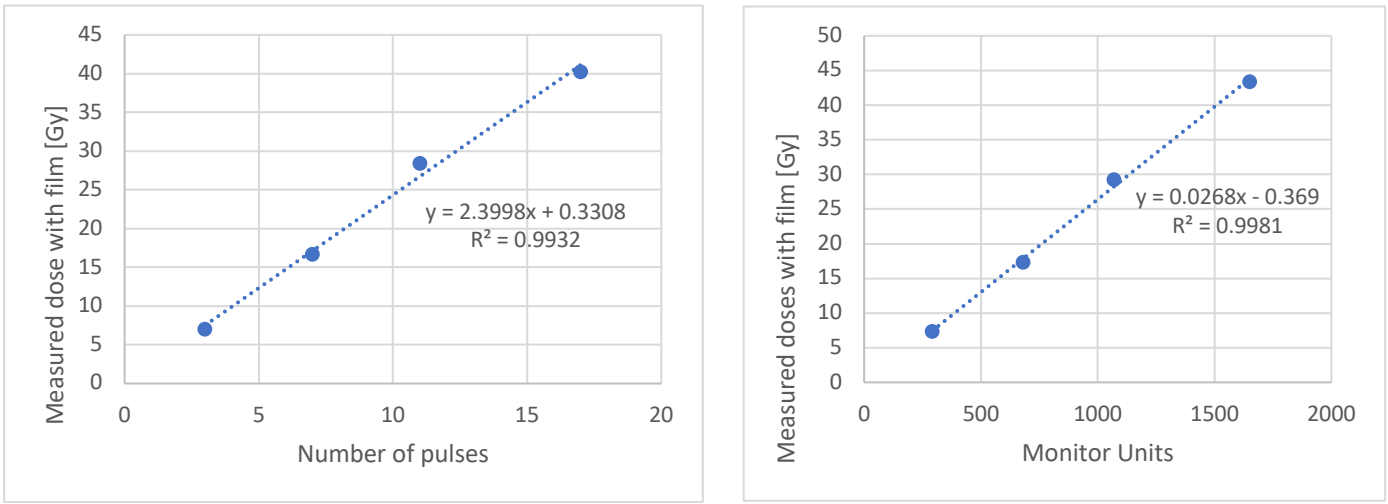

Figure 11: To the left, the dose measured with film as a function of number of pulses when irradiated with FLASH. To the right, the dose measured with film as a function of monitor units when irradiated with 10 MeV electrons at conventional dose rates.

5.3 Dose response linearity assessment

Linearity assessments were carried out for the R2 dose response results for all beam types investigated. The doses, up to which the gel response was linear, $R^2 \geq 0{,}98$, are shown in Figure 12 and Table 1. The doses when irradiating with 220 kV photons are calculated doses to the vials based on the setup used and in the case of the 10 MeV electrons at conventional dose rate and FLASH, the presented doses are the doses measured using film dosimetry. This is the case throughout this work. When more than one vial was irradiated with the same dose and the same radiation beam type the average R2 value was calculated.

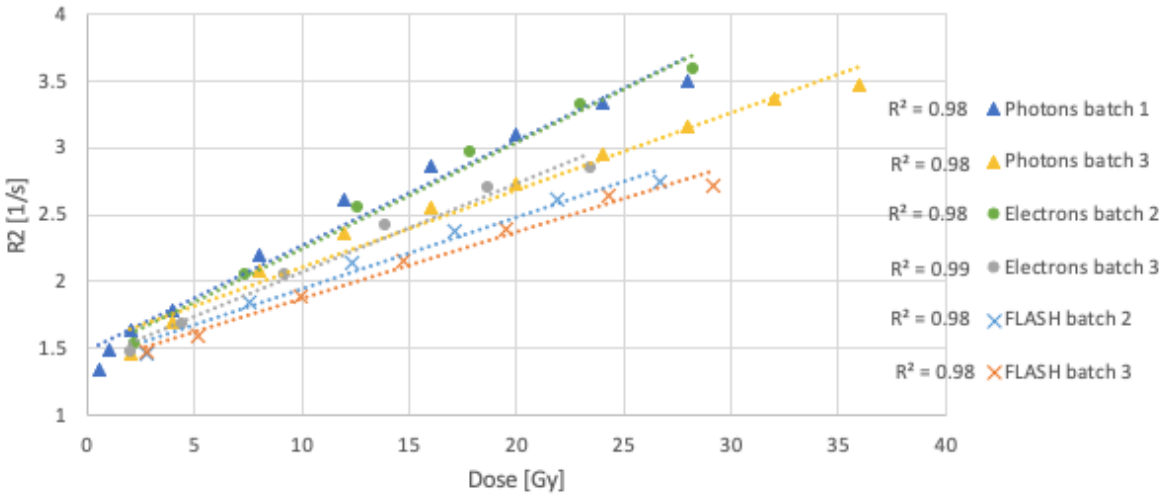

Figure 12: Plot of R2 as a function of dose showing the dose range where the gel response is linear, $R^2 \geq 0{,}98$

Table 1: The doses, up to which the gel response was linear for respective beam type					
220 kV photons		10 MeV electrons conv, dose rate		FLASH	
Batch 1	Batch 3	Batch 3	Batch 2	Batch 3	Batch 2
28 Gy	36 Gy	23 Gy	28 Gy	29 Gy	27 Gy

5.4 Dose response reproducibility

The mean R2 dose response when irradiated with 220 kV photons at 0.5, 2, 5 and 10 Gy is shown in Figure 13. Seven vials were irradiated at each dose level. Error bars of +/- SD are included and the exact data is presented in Table 2.

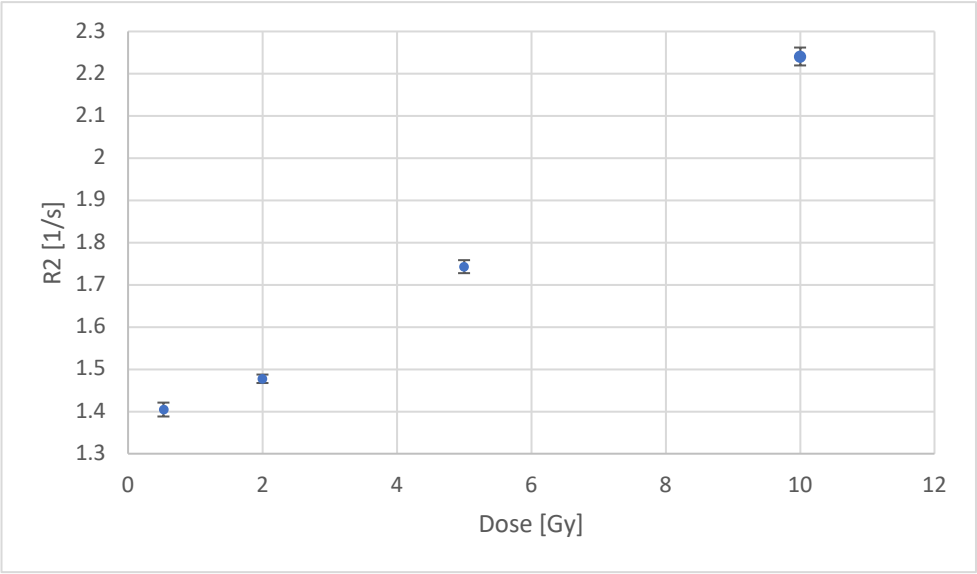

Figure 13: R2 mean dose response when irradiated with 220 kV photons at 0.5, 2, 5 and 10 Gy. Seven vials were irradiated at each dose level. Error bars of +/- SD are included.

Table 2: Dose, number of vials per dose level, mean R2 and SD for batch 0 when assessing intra batch variations			
Dose [Gy]	Number of vials	R2 [1/s]	SD [1/s]
0.53	7	1.405	0.016
2	7	1.477	0.010
5	7	1.743	0.015
10	7	2.231	0.021

5.5 Dose response for various beam types and dose rates

The irradiation scheme for the three batches of gel that were irradiated with 220 kV photons and/or 10 MeV electrons at conventional dose rate and/or FLASH is presented in Table 3.

Table 3: Irradiation scheme for batch 1-3					
Batch 1	Batch 2		Batch 3		
220 kV photons	10 MeV electrons conv. dose rate	FLASH	220 kV Photons	10 MeV electrons conv. dose rate	FLASH
2 vials per dose level	2 vials per dose level		1 vial per dose level		
Dose [Gy]	Dose [Gy]	Dose [Gy]	Dose [Gy]	Dose [Gy]	Dose [Gy]
0.5	2.7	2.3	2	2.0	2.7
1	7.5	7.4	4	4.4	5.1
2	12.3	12.6	8	9.2	9.9
4	17.1	17.8	12	13.9	14.7
8	21.9	23.0	16	18.7	19.5
12	26.7	28.3	20	23.5	24.3
16	31.5	33.5	24	26.4	29.1
20	36.3	38.7	28	33.0	33.9
24	41.1	43.9	32	37.7	38.7
28	-	-	36	42.5	43.5
32	-	-	40	47.3	-
36	-	-	-	-	-
40	-	-	-	-	-

The R2 dose response for batch 1, when irradiated with 220 kV photons from 0.5 up to 40 Gy is shown in Figure 14.

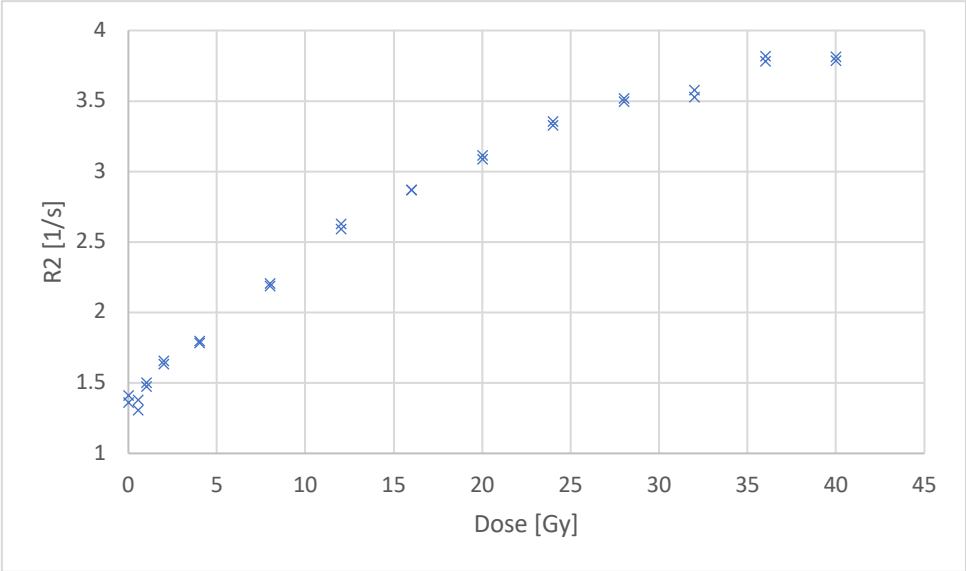

Figure 14: R2 dose response for batch 1 when irradiated with 220 kV photons. Two vials were irradiated with the same dose and therefore two data points are displayed at each dose level

The R2 dose response for batch 2, when irradiated with FLASH and 10 MeV electrons at conventional dose rate in the interval of around 2 to 44 Gy is shown in Figure 15.

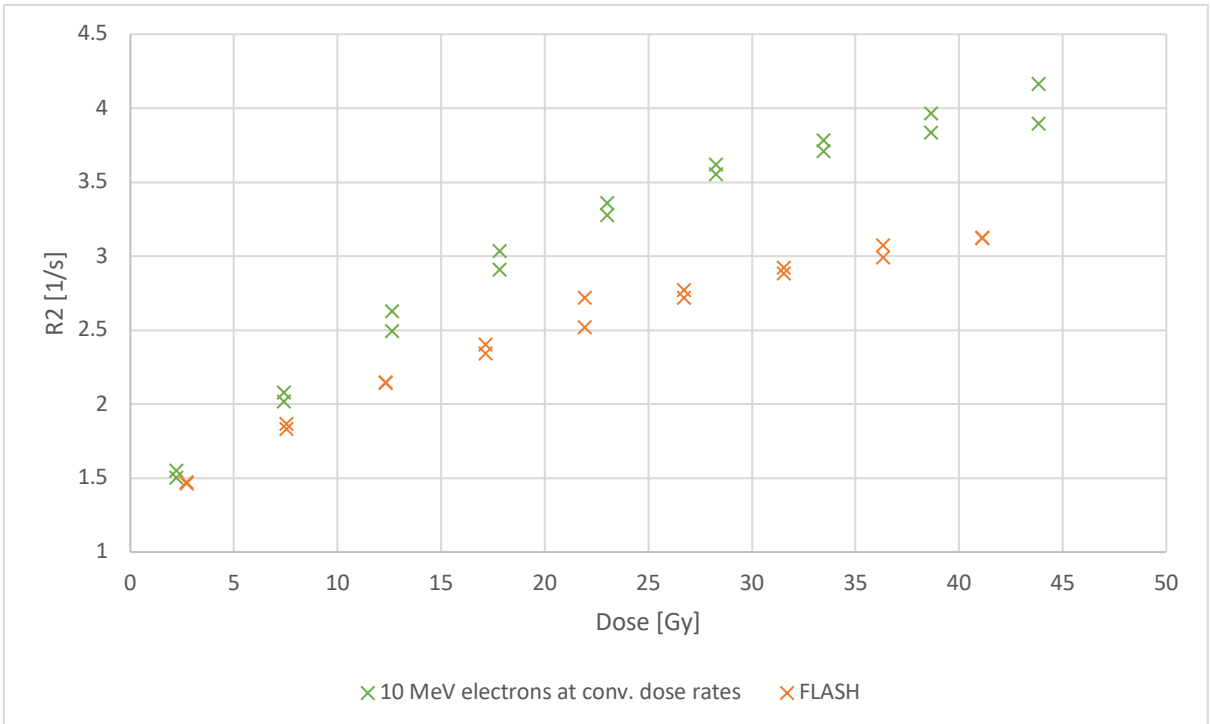

Figure 15: R2 dose response for batch 2 when irradiated with 10 MeV electrons at conventional dose rate and FLASH, in the interval of around 2 to 44 Gy. Two vials were irradiated with the same dose and therefore two data points are displayed at each dose level

The R2 dose response for batch 3, when irradiated with 220 kV photons, 10 MeV electrons at conventional dose rate and FLASH is shown in Figure 16.

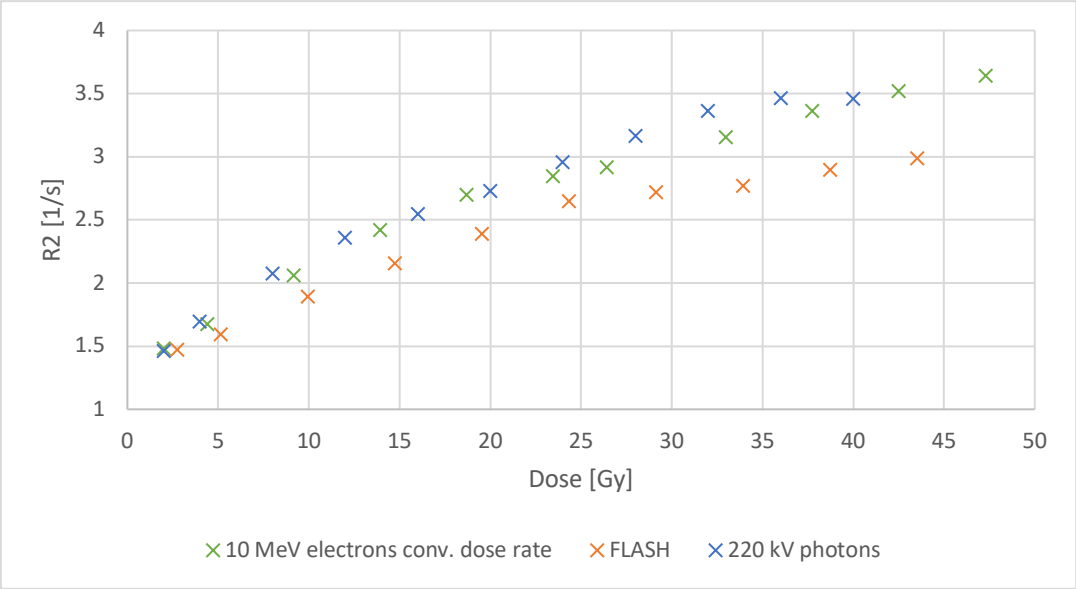

Figure 16: R2 dose response for batch 3 when irradiated with 10 MeV electrons at conventional dose rate, FLASH and 220 kV photons in the interval of around 2 to 47 Gy. Only one vial was irradiated at each dose.

5.6 Comparison within respective radiation beam type

For comparison, the gel response for each radiation beam type, 220 kV photons, 10 MeV electrons at conventional dose rate and FLASH, has been put into separate plots (Figure 17, 18 and 19). When more than one vial was irradiated with the same dose and the same radiation beam type the average R2 value was calculated.

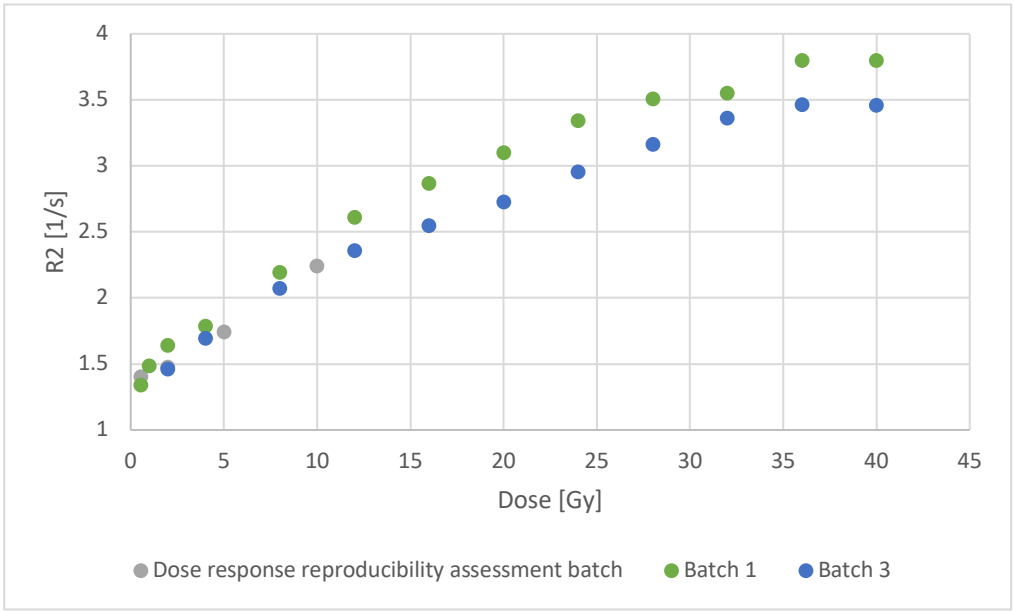

Figure 17: Comparison R2 dose response when irradiated with 220 kV photons

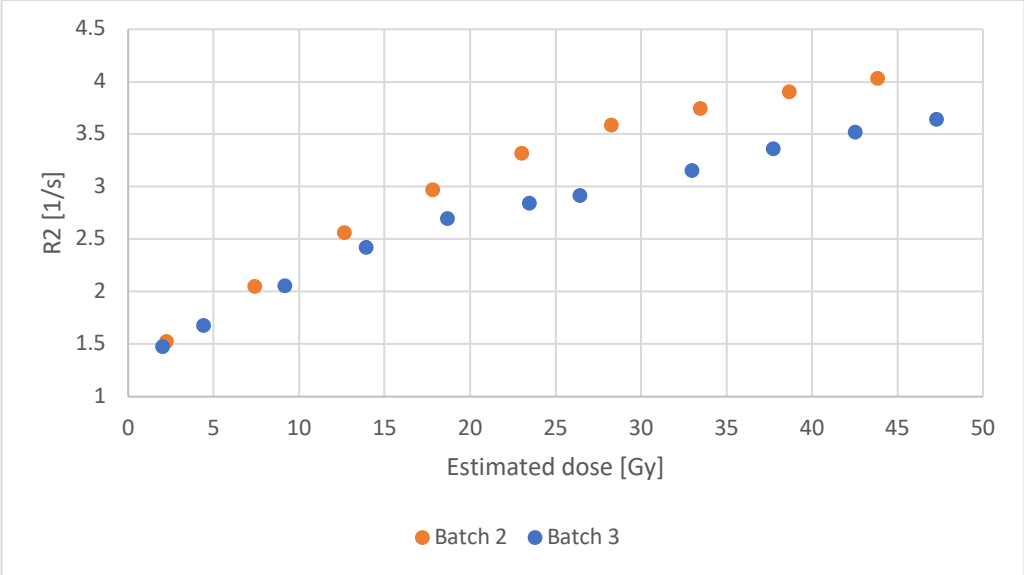

Figure 18: Comparison R2 dose response when irradiated with 10 MeV electrons at conventional dose rate

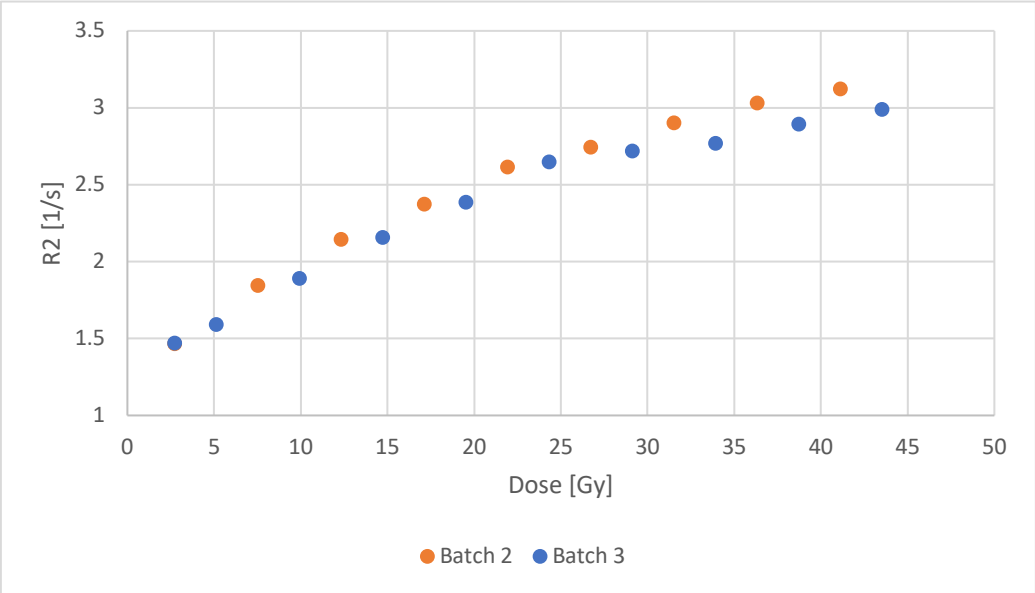

Figure 19: Comparison R2 dose response when irradiated with FLASH

The relative difference of R2 between the two batches of gel (Figure 17-19) is shown for all beam types in Figure 20.

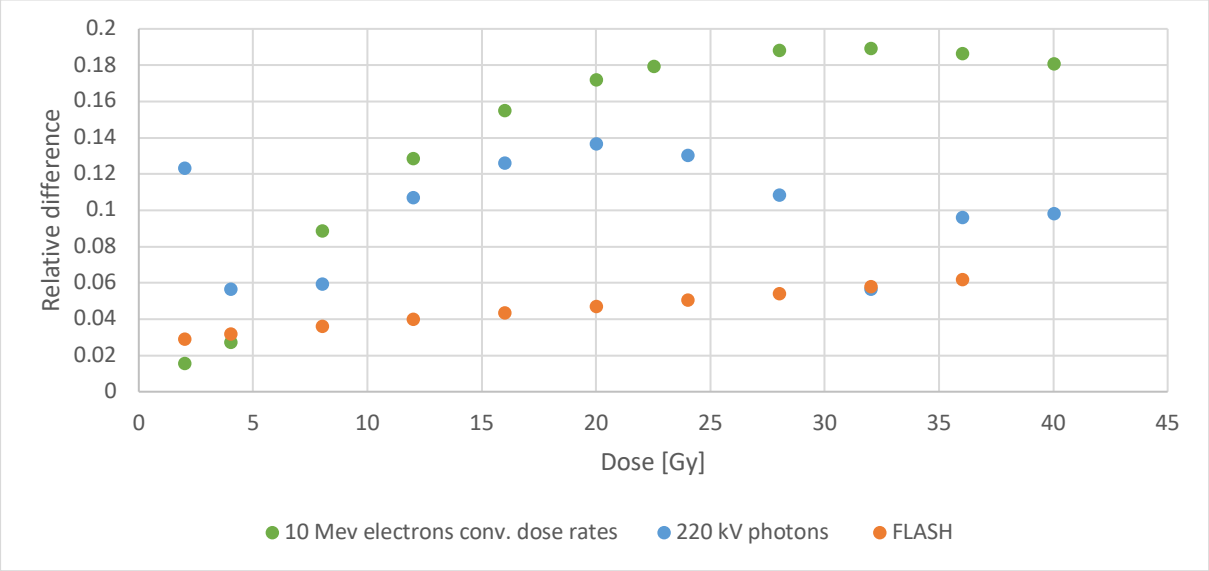

Figure 20: Relative difference of R2 between two batches of gel for all beam types investigated

5.7 Compiled dose response results

The R2 dose response results from all experiments within this study are presented in Figure 21. The average R2 value was used in the cases where more than one vial was irradiated with the same dose and the same radiation beam type.

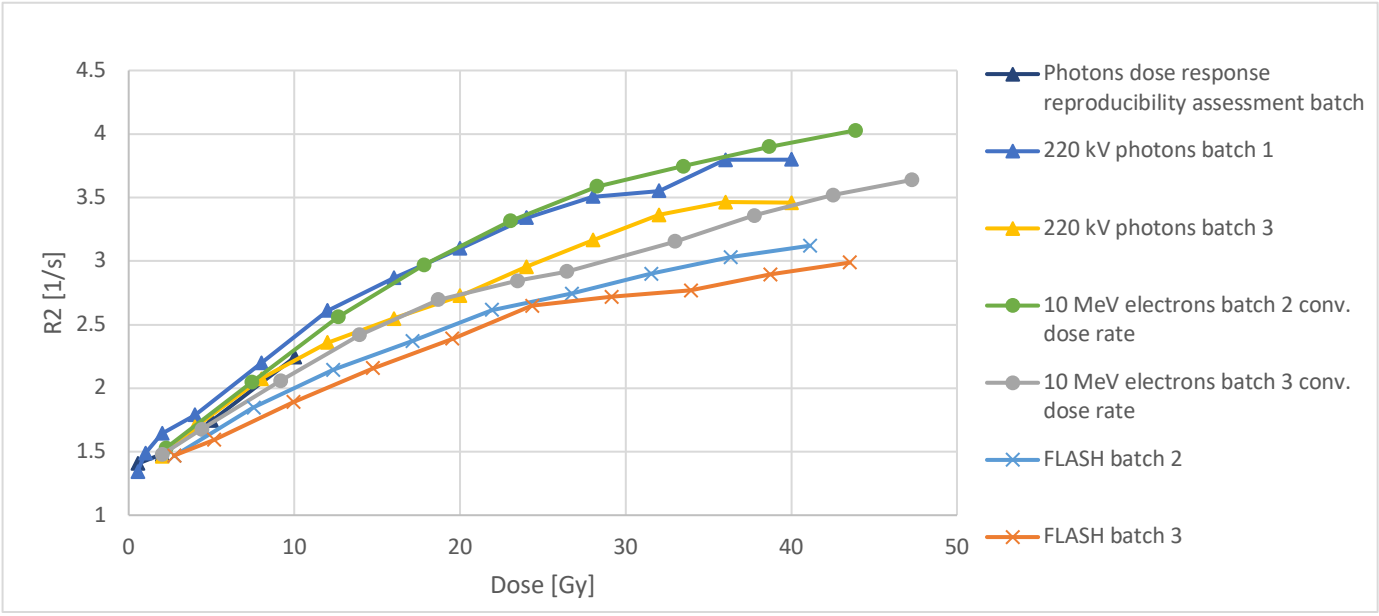

Figure 21: Compiled dose response results for all batches

6 Discussion and critical reflections

The startup of the new polymer gel laboratory is still in an early phase and as for now the stages from production to readout of the gel is still being optimized. Nevertheless, the creation of a gel dosimeter using MRI readout, relatively non-toxic ingredients and a simplified mixing procedure can be seen as successful since most of the obtained results goes in line with results from previous studies including R2 values within reasonable levels and a linear dose response at low doses, here up to at least 23 Gy. However, it should be acknowledged that two additional experiments, not presented in this thesis, resulted in deviating and unexpected results. The cause of these results is not fully understood and even though the main hypothesis does not point towards the simplified mixing procedure or the content of the gel, it cannot be excluded with complete certainty.

Comparison of the two different evaluation approaches of obtaining R2 values was made for one batch only since the results from the two approaches had very good agreement. The results from investigating intra-batch variations, with respect to the dose response reproducibility, gave a standard deviation (SD) of the R2 relaxation rate between 0.010-0.021 for R2 values between 1.405 and 2.231. A result indicating high reproducibility and goes in line with a previous study [4]. The dose response reproducibility assessment was made for doses up to only 10 Gy and not higher due to the limitation in number of vials. Furthermore, the results from batch 2, Figure 15, indicates that the dose response reproducibility decrease at very high doses for 10 MeV electrons at conventional dose rates. The same result is however not observed when irradiated with FLASH within the same batch. The investigation of the difference between experiments indicates inter-batch variations. The largest relative difference of up to 19 % is observed for the 10 MeV electrons at conventional dose rate and the smallest of up to around 6 % is observed for FLASH. The relative difference is mainly increasing in the whole dose interval in both cases, but for 220 kV photons it variates. Inter-batch variations were however expected since gel dosimeters are not absolute dosimeters. Nevertheless, the observation highlights the need of a calibration for each batch of gel.

When irradiated with 220 kV photons, the gel dose response indicates linearity up to 28 Gy in one case and up to 36 Gy in the other, both with R^2 values above 0.98. It should be noticed that low doses of 0.5 and 1 Gy are only included in the case where the gel showed linearity up to 28 Gy, which is probably why the result differs. A R^2 value of 0.98 to show linearity was chosen based on previous work [18]. When irradiated with 10 MeV electrons at conventional dose rate and FLASH the gel dose response is instead linear up to about 23 and 28 Gy, and 27 and 29 Gy respectively for the two different batches. However, the gel response from the 10 MeV electrons at conventional dose rate does not show the same distinct refraction from linearity at doses around 20 Gy as in the case of FLASH, observed in Figure 21. The aggregated result indicates that the NIPAM gel is linear at least up to 21 Gy for all radiation beam types used.

The comparison of the tree different beam types indicates that when irradiated with FLASH the lowest gel dose response is obtained. This observation agrees with observations made in a previous study, that a lower dose response is obtained with increasing dose rate [2]. It can also be observed that when irradiated with photons and electrons at conventional dose rate, the gel gives similar dose response within the same batch of gel. This could however only be concluded in one experiment since only one such experiment was made.

Initially, vials without exposure to radiation were included in the results. Relative to the R2 values of vials exposed to radiation, the R2 values in these unexposed vials within the same

batch of gel, were too high for a linear dose response relationship. The cause of the high R2 values was possibly originating from the high signal in these unexposed vials which caused artifacts to arise in the MR image. Since the artifacts propagated in the phase-encoding direction the artifacts resulted in lower signal in the vials that were MRI scanned in the same row as the unexposed vials. The consequence of the decreased signal was increased R2 values. This phenomenon occurred when unexposed vials were placed in the same row, and it was more widespread with more unexposed vials in that row and at some specific TE_{eff}. This observation is clearly also visible for vials exposed to very low doses, around 0.5 Gy, since these vials also possess high signals. This is probably the explanation for the slightly too high R2 values in experiment A for vials exposed to 0.5 Gy. Because of the described observation, unexposed vials were excluded from all results in all experiments. Though, it must be kept in mind that unexposed vials were still scanned in every experiment which might have affected the result for vials scanned in the same row as these vials. A MR image, Figure A, where these artifacts appear is attached in the appendix.

For batch 1, the R2 values of the vials exposed to doses below 1 Gy are instead too low for a linear relationship. In batch 1, only two unexposed vials were scanned whereas in the batch where the dose response reproducibility was assessed there were four. Nevertheless, for both cases they were all scanned in the same row. Due to that only two unexposed vials were scanned in batch 1, the above described cause to why the R2 values were too high, does not make an impact here. This might explain why the values are not too high, however it does not explain why they are too low. Thus, this must be further investigated.

Two gel experiments within the frame of this master thesis work were removed due to difficulties to explain the results. The main hypothesis for the result of the first unusable experiment is that the large amount of gel that was prepared made it impossible for the magnetic stirrer to mix the content properly. Because of this, the content was not evenly distributed which led to deviating results. The main hypothesis for the deviating result in the second of the two omitted experiments is that the MR readout technique in this experiment was made with a slice thickness of 5 mm instead of 10 mm. Due to the decreased SNR with decreased slice thickness and the large ETL, the artifacts just described originating from high signals, emerged clearer in these images. One way to decrease the impacts from these artifacts would be to exclude vials exposed to doses lower than 1 Gy from the MR scanning procedure all together. The reason of using a slice thickness of 5 mm instead of 10 mm was that vials exposed to 5x5 mm small 220 kV photon fields (explained in appendix) were scanned at the same time. To avoid the same problems in the experiment where the dose response reproducibility was assessed and 5x5 mm filed vials were scanned simultaneously, the vials were scanned using both 5 mm and 10 mm slice thickness. The images with 10 mm slice thickness were used for the open field irradiated vials and the images with 5 mm slice thickness were used for the vials irradiated with 5x5 mm field. Thus, the problem remained for the images used for the 5x5 mm vials.

The MRI parameters used in this thesis were chosen based on previous work [18]. However, due to updates made on the MR scanner, the exact same setting could not be used. Efforts were made to obtain as similar settings as possible but while doing so, various of problems occurred. For example, to obtain the same range of TE_{eff}, the receiver bandwidth had to be decreased. With decreased receiver bandwidth the sensitivity for changes in the magnetic field increases and susceptibility artifacts becomes more tangible. Susceptibility artifacts are geometrical distortions that arise at the interface of volumes with differences in magnetic susceptibility, which in this specific case arose at the interface between the glass of the vial and the surrounding air. Nevertheless, the impact of these artifacts on the results were excluded by

placing the ROIs at a distance from the edges of the vials. Adjustments were made on many of the other settings to minimize artifacts and noise but due to lack of time, adjustments were not made to a full extent.

7 Conclusions

It was feasible to use relative non-toxic ingredients (NIPAM), MRI-readout, and a simplified mixing procedure with tap water under normal oxygen levels to obtain a gel dosimeter with linear dose response up to at least 23 Gy. The small intra-batch variations found indicated a very high dose response reproducibility while the larger inter-batch variations underlined the need for calibration of each gel batch. The gel exhibited linearity of the dose response up to at least 23 Gy for all three radiation beam types investigated. A lower gel dose response was observed when irradiated with FLASH compared to irradiation with 220 kV photons or 10 MeV electrons at conventional dose rates.

8 Future perspectives

- To investigate why the dose response from FLASH is linear up to only around 20 Gy. Does it have to do with the fact that the FLASH effect is observed around this specific dose level? This is especially interesting since the gel is tissue equivalent.

- To assess the dose response reproducibility for doses higher than 10 Gy and for all radiation beam types.

- To evaluate how many MR images that are required to obtain an appropriate R2 result i.e., if fewer than sixteen.

- To optimate the MR sequence to a lager extent than in this thesis project.

- To investigate if a shorter scan time can be used, if for example, artificial intelligence (AI) is used to reduce artifacts and noise.

- To investigate the variations in R2 between experiments by making many different gels and expose them to the same dose levels.

- To investigate the theory that the placement of the vials in the MR scanner affects the results i.e., the presence of many unexposed vials in the same row.

- To further investigate the dose response at doses below 2 Gy when using 220 kV photons. This is particularly important since the accuracy at low doses are of great importance to spare normal tissues.

- To investigate potential dose response variations in various parts of the vial.

- To use a scale with more accurate readability than 1.0 g when manufacturing the gel and investigate if an excessive amount of THPC affects the result.

- To investigate the possibility to use this novel gel dosimeter for 2D and 3D absorbed dose measurements. A first approach has been carried out using 5x5 mm 220 kV photon beams (Appendix).

9 References

[1] Farhood, B., Geraily, G. and Abtahi, S., 2019. A systematic review of clinical applications of polymer gel dosimeters in radiotherapy. *Applied Radiation and Isotopes*, 143, pp.47-59.

[2] Waldenberg, C., Karlsson Hauer, A., Gustafsson, C. and Ceberg, S., 2017. Dose integration and dose rate characteristics of a NiPAM polymer gel MRI dosimeter system. *Journal of Physics: Conference Series*, 847, p.012063.

[3] Ceberg, S., 2010. 3D Verification of Dynamic and Breathing Adapted Radiotherapy using Polymer Gel Dosimetry. Medical Radiation Physics. Department of Clinical Science, Malmö. Lund University. Lund.

[4] Ceberg, S., Gagne, I., Gustafsson, H., Scherman, J., Korreman, S., Kjær-Kristoffersen, F., Hilts, M. and Bäck, S., 2010. RapidArc treatment verification in 3D using polymer gel dosimetry and Monte Carlo simulation. *Physics in Medicine and Biology*, 55(17), pp.4885-4898.

[5] Baldock, C., De Deene, Y., Doran, S., Ibbott, G., Jirasek, A., Lepage, M., McAuley, K., Oldham, M. and Schreiner, L., 2010. Polymer gel dosimetry. *Physics in Medicine and Biology*, 55(5), pp.R1-R63.

[6] McAuley, K. and Nasr, A., 2013. Fundamentals of gel dosimeters. *Journal of Physics: Conference Series*, 444, p.012001.

[7] Nitz, W. and Reimer, P., 1999. Contrast mechanisms in MR imaging. *European Radiology*, 9(6), pp.1032-1046.

[8] Demangeat, J., 2013. Nanosized solvent superstructures in ultramolecular aqueous dilutions: twenty years' research using water proton NMR relaxation. *Homeopathy*, 102(2), pp.87-105.

[9] Berglund, E. and Jönsson, B., 2007. *Medicinsk fysik*. Lund: Studentlitteratur, pp.109-113.

[10] Mugler, J., 2014. Optimized three-dimensional fast-spin-echo MRI. *Journal of Magnetic Resonance Imaging*, 39(4), pp.745-767.

[11] Whitney, H., Gochberg, D. and Gore, J., 2006. Magnetization transfer in polymer gel dosimeters. *Journal of Physics: Conference Series*, 56, pp.253-255.

[12] Cheng, K., Hsieh, L. and Shih, C., 2016. A Comprehensive Evaluation of NIPAM Polymer Gel Dosimeters on Three Orthogonal Planes and Temporal Stability Analysis. *PLOS ONE*, 11(5), p.e0155797.

[13] Xstrahl.com. 2022. [online], Xstrahl Life Science. Atlanta, Georgia. Available at: <https://xstrahl.com/wp-content/uploads/2020/05/Xstrahl-XenX-Brochure.pdf> [Accessed 6 January 2022].

[14] Hughes, J. and Parsons, J., 2020. FLASH Radiotherapy: Current Knowledge and Future Insights Using Proton-Beam Therapy. *International Journal of Molecular Sciences*, 21(18), p.6492.

[15] Lempart, M., Blad, B., Adrian, G., Bäck, S., Knöös, T., Ceberg, C. and Petersson, K., 2019. Modifying a clinical linear accelerator for delivery of ultra-high dose rate irradiation. *Radiotherapy and Oncology*, 139, pp.40-45.

[16] Konradsson, E., Ceberg, C., Lempart, M., Blad, B., Bäck, S., Knöös, T. and Petersson, K., 2020. Correction for Ion Recombination in a Built-in Monitor Chamber of a Clinical Linear Accelerator at Ultra-High Dose Rates. *Radiation Research*, 194(6).

[17] Ervin B. Podgorsak., 2016. *Radiation Physics for Medical Physicists.* Third Edition. Springer. pp. 801-812.

[18] Waldenberg, C. *Characterization and evaluation of a NIPAM polymer gel MRI dosimeter system.* Thesis project. The Sahlgrenska academy. University of Gothenburg. 2015

Appendix

Artifacts MR image

Artifacts appearing in the MR image possibly caused by the high signal in the unexposed vials are shown in Figure A.

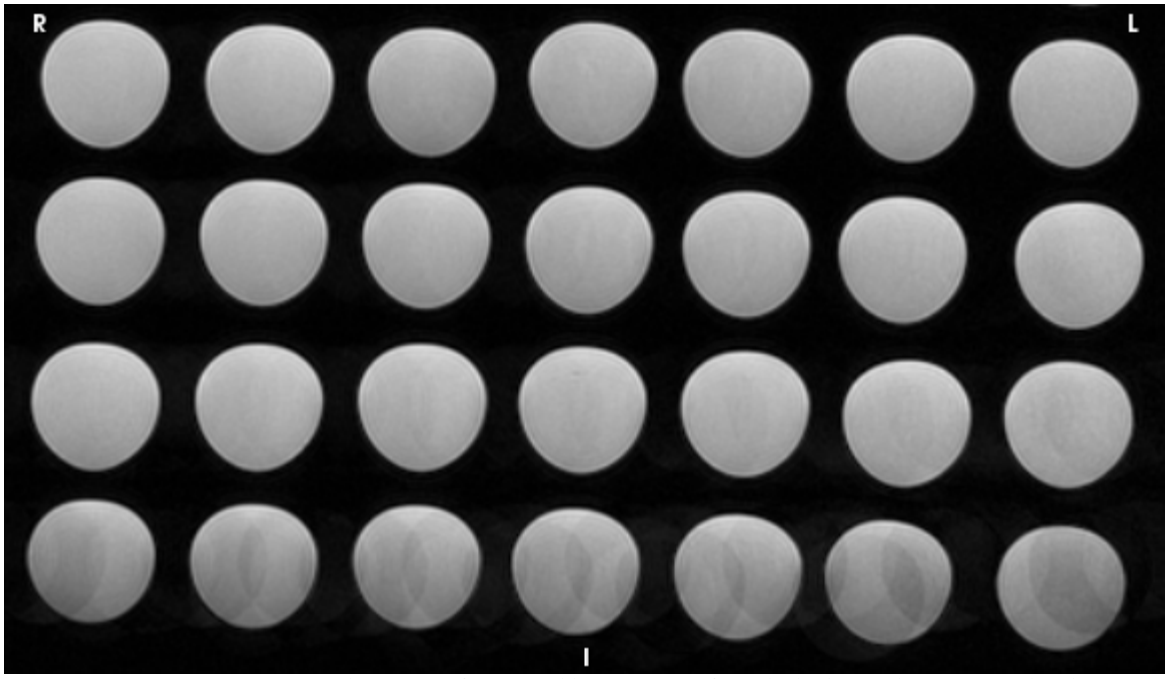

Figure A: MR image showing artifacts possibly originating from the high signal in unexposed vials

220 kV photons small fields

Additional to the irradiations already presented in this master thesis, vials were irradiated with 220 kV photons using 5x5 mm small fields. The irradiation scheme is shown in Table A. The same settings were used as previously described for irradiation with 220 kV photons, but with an additional collimator forming a 5x5 mm field. Here, the vials were placed such that ISO center would be as close as possible to the central axis of the vial but one third from the bottom of the vial. This position resulted in a SSD of 34 cm. Instead of the XenX irradiator platform, a narrow gutter was used to hold the vials in place (Figure B).

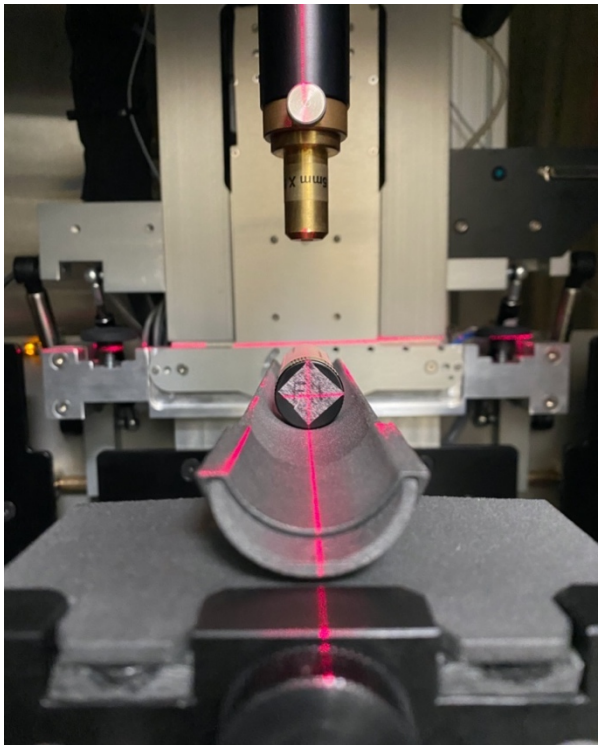

Figure B: The setup used when irradiated with 220 kV photons using 5x5 mm small fields

Table A: Irradiation scheme when irradiating with small 5x5 220 kV photon fields					
Number of fields	Gantry angle field 1 [°]	Gantry angle field 2 [°]	Gantry angle field 3 [°]	Dose per field [Gy]	Dose in the overlap [Gy]
2	0	90	-	5	10
3	0	135	225	2	6

During MRI scanning of the 5x5 mm fields, the exact same settings were used as presented in the method except that the slice thickness was set to 5 mm instead of 10 mm and the center of the slice was placed as close to the center of the 5x5 mm field as possible. The changed slice thickness resulted in slightly changed TE_{eff} but with a deviation of less than 1 %. Additional to the six vials, the vials irradiated with open fields in the dose response reproducibility assessment (the same batch of gel) were scanned simultaneously and hence scanned twice. From the obtained MR images, a T2 map was obtained in MICE toolkit. With ROIs similarly placed and shaped as previously described, now made in ImageJ 1.53k bundled with Java 1.8.0_172 https://imagej.nih.gov/ij/download.html, the average T2 of each vial irradiated with open fields was calculated. The average T2 as a function of dose was plotted and a calibration curve was obtained by linear curve fitting (Figure C). In ImageJ, profiles that crossed the middle of the vials were drawn (Figure D), from 180° to 0° relative to how they were irradiated and with the obtained calibration curve the dose in each pixel along each profile were calculated.

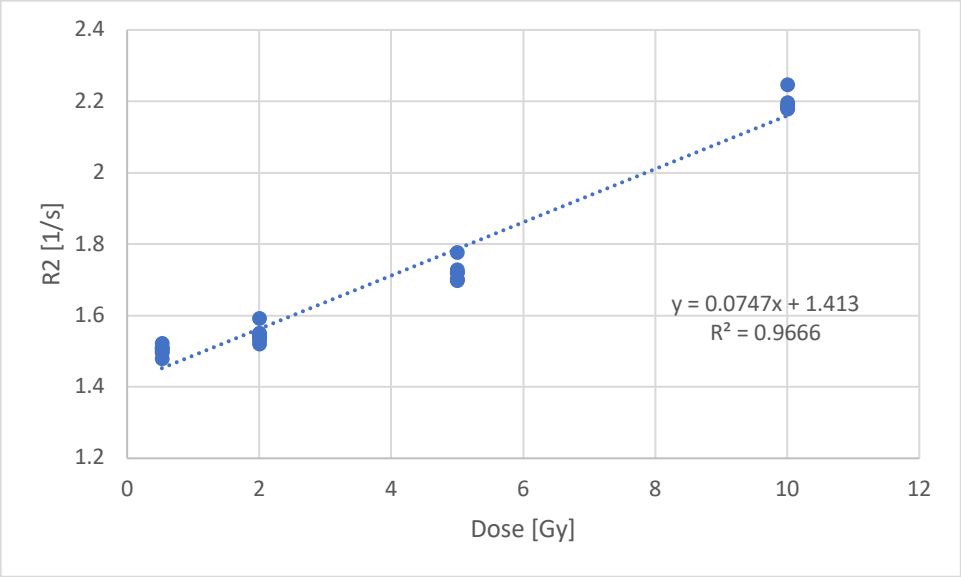

Figure C: The calibration curve of R2 as a function of dose.

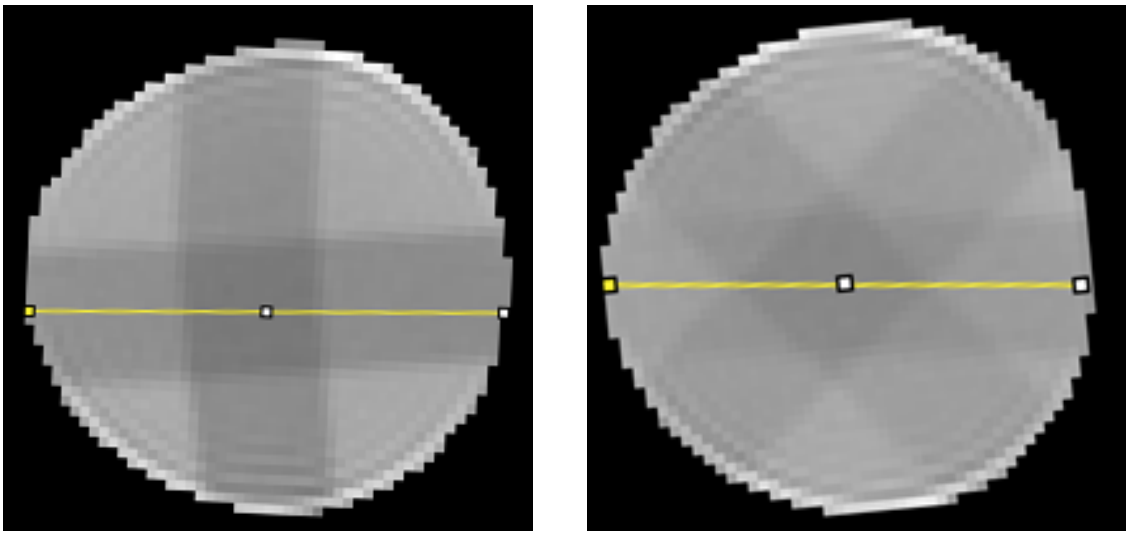

Figure D: To the left, MR image of the vial irradiated with two 5x5 mm fields. To the right, MR image of the vial irradiated with 3 5x5 mm fields. Yellow line indicates the positioning of the profiles

The treatment planning system for the XenX, Micro RayStation 8B, was used to make two individual dose plans for the vials irradiated with 5x5 mm fields. One dose plan was made with tree fields and one with two fields (Figure E and F). A vial containing gel was simulated in the program. The density for the glass was set to 2.33 g/cm^3, since the actual density of the glass closer to 2.5 g/cm^3, was not available. The density of the gel was set to one, as water. The SSD was set to 34 cm as during irradiation. The fields were slightly shifted from the center of the vial to better resemble the positioning of the fields in the MR image. A profile that crossed the middle of the vial (middle of the field), from 180° to 0° relative to how they were irradiated, was made in each vial. The relative doses of the profiles obtained from the MR images were compared to the relative doses of the profiles obtained with Micro RayStation 8B (Figure G and H).

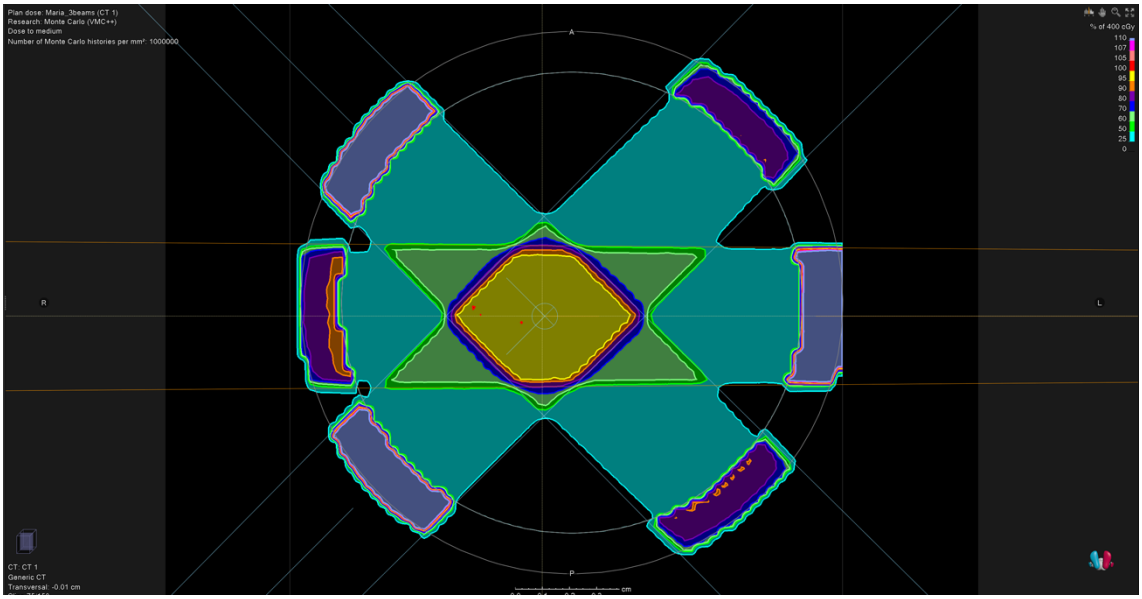

Figure E: Dose plan obtained in Micro RayStation 8B using three fields with gantry angles 0°, 135°, and 225°. The image is rotated 90° to the right

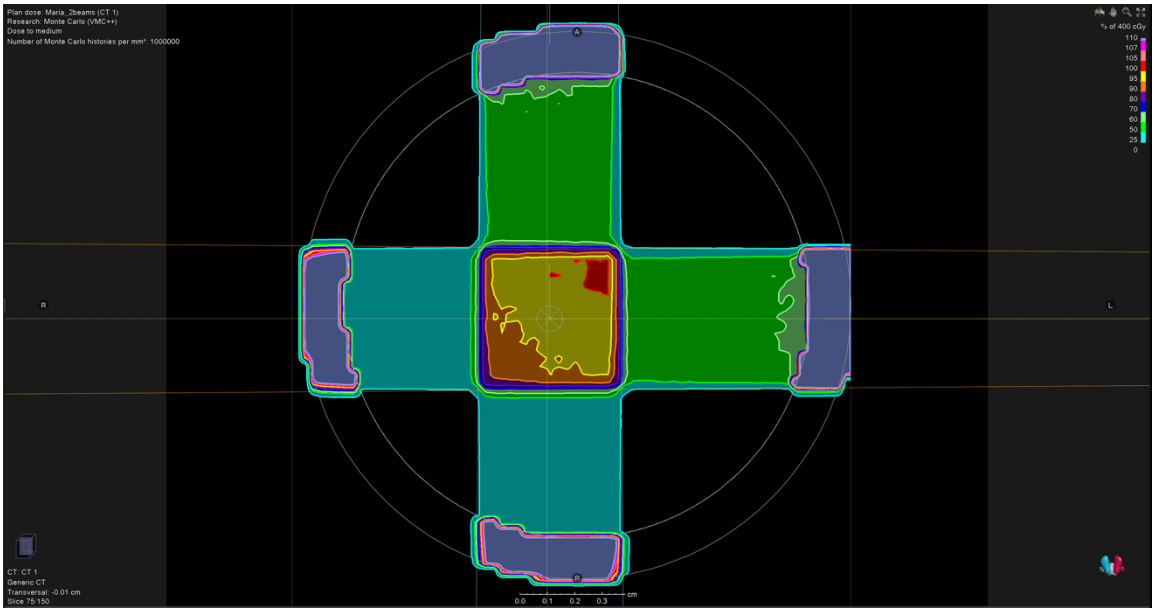

Figure F: Dose plan obtained in Micro RayStation 8B using two fields with gantry angles 0° and 90°. The image is rotated 90° to the right

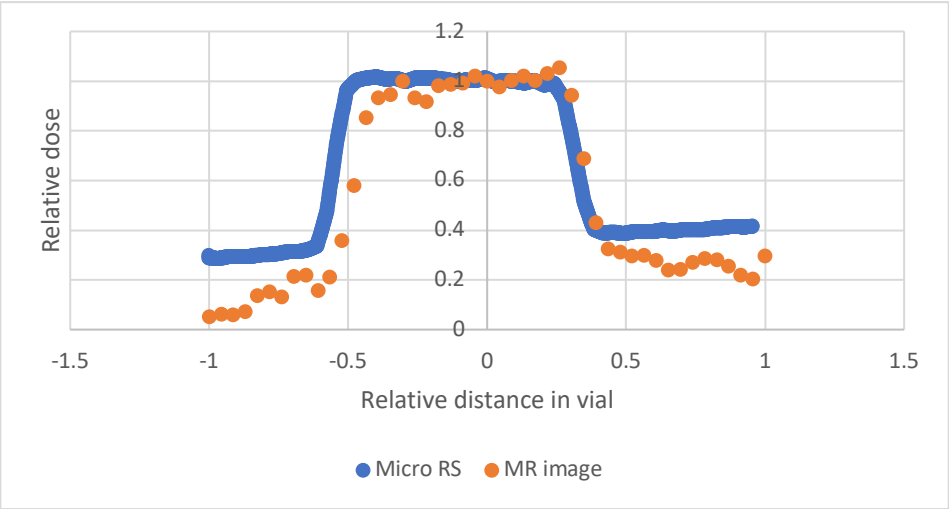

Figure G: Relative dose profiles for three 5x5 mm fields obtained using Micro RS and from MR image

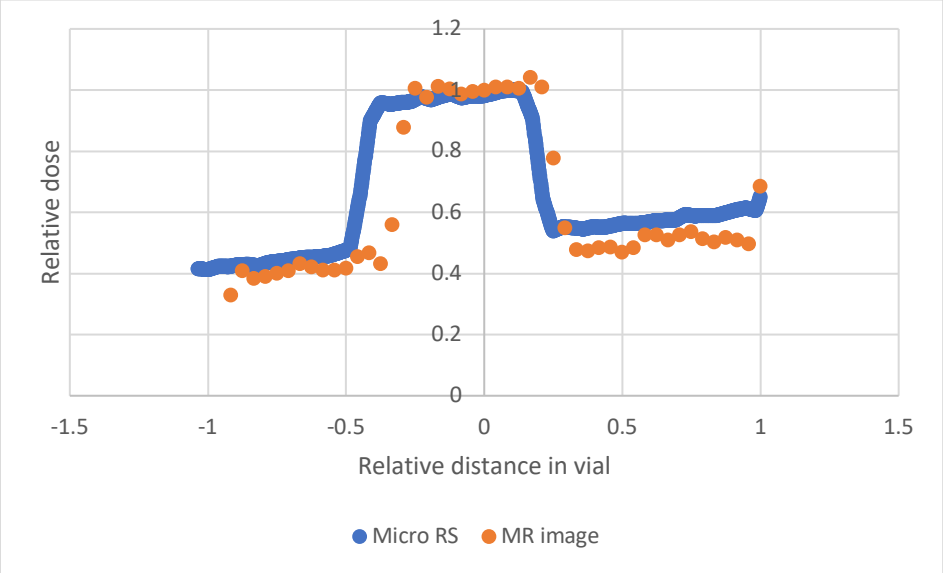

Figure H: Relative dose profiles for two 5x5 mm fields obtained using Micro RS and from MR image

From Figure G and H it can be observed that the relative doses of the profiles obtained from the MR images and the relative doses of the profiles obtained with Micro RayStation 8B agrees to some extent. However, it can be observed that there is a shift in the overlap. In the case of three 5x5 mm fields, it can also be observed that the relative dose in areas where the fields does not overlap differs quite a lot. Additionally, it can be observed that the inclination in areas where all three fields overlap differs in the two cases. In the case of two 5x5 mm fields, the overall agreement is better, however a shift is still observed.

The reason the profiles doesn't agree better could be that the fields are not in the exact same position in the two cases. Another possible reason is that the calibration curve obtained is not optimal since a slice thickness of 5 mm was used instead of 10 mm (as explained in the discussion). Further investigations must be made in order to be able to make any conclusions about the agreement and for a gamma analysis to be relevant to make.

10 Acknowledgments

I would like to express my gratitude to all my supervisors **Sofie Ceberg**, **Christian Jamtheim Gustafsson**, **Crister Ceberg** and **Sven Bäck** who made it possible for me to do such a wide and interesting master thesis covering dosimetry, external radiation therapy and magnetic resonance imaging (MRI). Thank you for sharing your invaluable expertise within these fields.

A special thank you to **Sofie Ceberg**, my main supervisor, who guided and supported me a little extra during this period. Sofie, you really inspired me and got me excited about gel dosimetry, a topic which I know is close to your heart. **Christian Jamtheim Gustafsson**, thank you for making it possible to use MRI as the readout technique in this thesis project. I'm grateful that you were never afraid of giving me comments and feedback which has increased my knowledge within MRI and developed my overall way of writing. **Crister Ceberg**, I really appreciate all your help and especially for the time requiring help you gave me at the beginning of the project to irradiate at the XenX. You made the waiting time in between irradiations fun and inspiring by sharing your story of becoming a medical physicist. **Sven Bäck**, I am grateful for your general support and for always bringing new perspectives to the table.

I'm also extremely grateful to **Elise Konradsson**, who with her expertise within FLASH and film dosimetry helped me a lot in my project. Thank you for all your help and for dedicating time for me and my project. I would also like to give a warm thank you to **Patrik Brynolfsson** from MICE toolkit who made sure that a new version of the program was released such that I could obtain T2 maps for my non-human data. Your friendly accommodating and insider tips about MICE were really appreciated.